JOURNAL OF GEOPHYSICAL RESEARCH, VOL. 100, NO. B8, PAGES 15,351–15,372, AUGUST 10, 1995

Evidence for a role of the downgoing slab in earthquake slip partitioning at oblique subduction zones

Xinping Liu[1] and Karen C. McNally
Institute of Tectonics, University of California, Santa Cruz

Zheng-Kang Shen
Department of Earth and Space Sciences, University of California, Los Angeles

Abstract. A new model, incorporating shear deformation within a subducting slab, is proposed to explain slip partitioning for oblique plate motion at subduction zones. On the basis of investigation of 450 interplate earthquakes at 24 subduction zone segments we find that the degree of slip partitioning is largely correlated with the calculated slab pull force. Such correlation suggests that other than the upper plate deformation, the slab pull force plays an important role in controlling oblique subduction. Our model proposes that the force balance between the slab pull force, the interplate coupling resistance, and the viscous mantle drag (the latter two are passive forces to the former one) produces a lateral shear within the slab, which causes the slab to deform and change its motion direction gradually toward trench normal as it subducts. The amount of direction change, which would be observed as the slip partitioning during earthquakes, therefore is closely related to the major plate driving force at the subduction zone, which is the slab pull force in our model.

Introduction

Almost all major segments of circum-Pacific subduction zones (Figure 1) are undergoing oblique subduction, which causes along strike deformation at the subduction zones. The interplate earthquakes provide information about such deformation. It is often observed that the slip vectors of interplate earthquakes deviate from the plate motion directions toward the directions normal to the trench [*Fitch*, 1972]. This has been explained by partitioning of plate motion between slip across the interplate boundary and intraplate deformation within the overriding plate which may involve forearc shear faulting and back arc spreading [*Fitch*, 1972; *Beck*, 1983, 1986, 1991; *Walcott*, 1978; *Michael*, 1990; *Jarrard*, 1986a; *Ekström and Engdahl*, 1989; *McCaffrey*, 1990, 1991, 1992; *Jones and Wesnousky*,1992; *Dewey*, 1980].

Forearc shear faults are usually located about 100–300 km from the trench line and often involve arc parallel strike-slip faulting [*Jarrard*, 1986a]. *Jarrard* [1986a,b] suggested that the major factors controlling forearc shear faulting at oblique subduction zones are the convergence obliquity, the strength of the overriding plate, and the degree of interplate coupling. Various mechanical models have been proposed to quantify the relationship between the partitioning of slip between interplate earthquakes and along forearc shear faults, as a function of the forces applied on the forearc plate [i.e., *Beck*, 1991; *McCaffrey*, 1992]. The tectonic setting of the subduction zone is shown in Figure 2. Section a is the oceanic plate before subduction, section b the forearc or sliver plate (defined as the part of the overriding plate bounded by the forearc shear faults and the subducting slab), section c the upper plate, and section d the subducting slab. Using an approach of force balance on the sliver plate, *McCaffrey* [1992] argued that if plate convergence obliquity is less than a critical angle, the arc parallel shear force will not be large enough to cause motion on forearc shear faults, so that relative plate motion of section a to section c ${}_a\vec{V}_c$ is equal to ${}_a\vec{V}_b$, since ${}_b\vec{V}_c$ is zero. If the relative motion ${}_a\vec{V}_d$ has no along strike component and the earthquake slip vectors are representative to the in situ relative plate motion, ${}_a\vec{V}_b$ equals to a pure bending ${}_a\vec{V}_d$ plus the earthquake slip vector ${}_d\vec{V}_b$. On the basis of such a model, *McCaffrey* found that the critical value for convergence obliquity for Sumatra is about $20°\pm5°$ and $25°-45°$ for the Aleutians. In a following paper, *McCaffrey* [1993] generalized his model by introducing viscous components into describing the forearc slip, but it is an open question whether the material of the earth would deform in the ways his models suggested. In the following discussion

[1]Now at Institute of Geophysics and Planetary Physics, University of California, Los Angeles.

Paper number 95JB00870.
0148-0227/95/95JB-00870$05.00

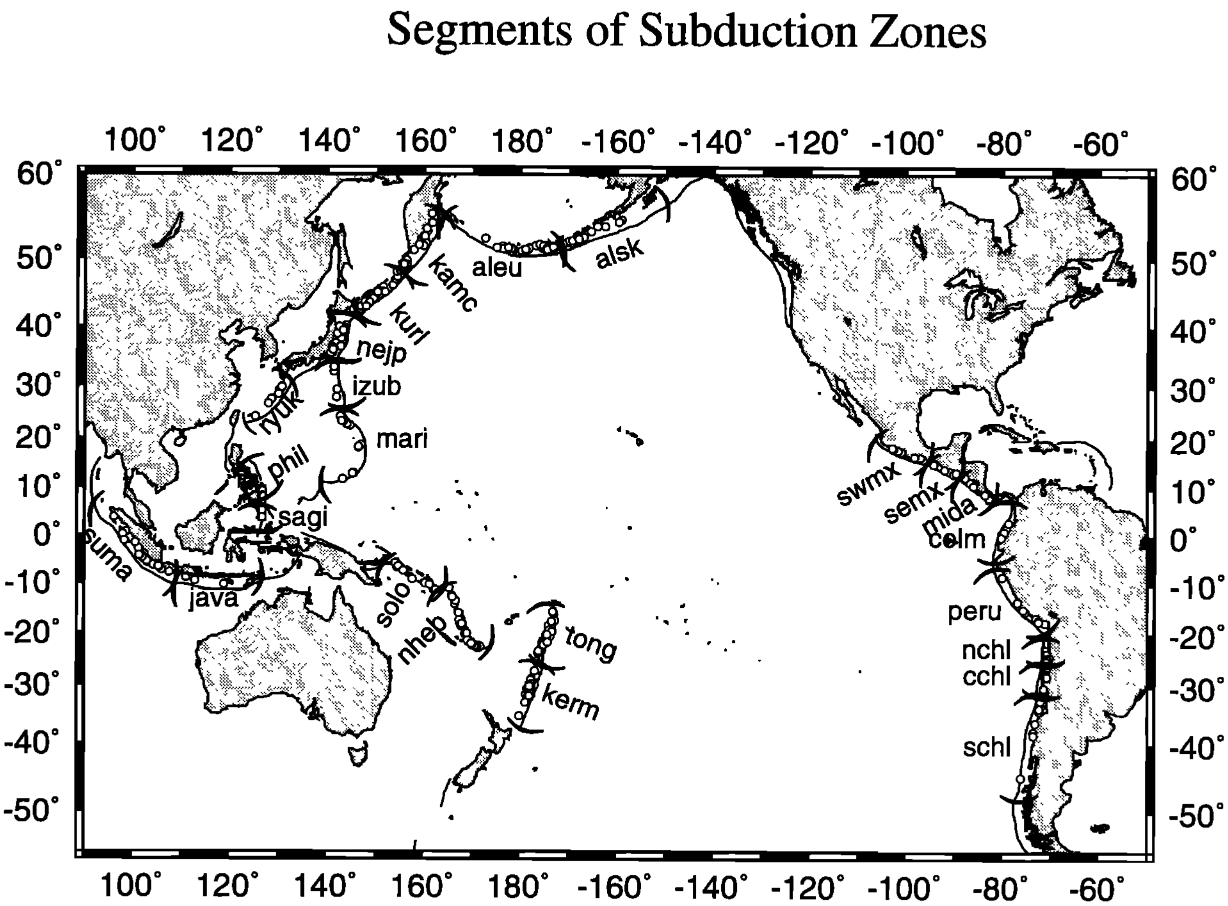

Figure 1. Major segments of subduction zones used in this study. The full name of each subduction zone segment is listed in Table 1. Open circles are selected interplate earthquakes.

we will mainly concentrate on his 1992 work as a representation of the forearc deformation models.

Forearc shear faults are likely important for some oblique convergence zones, but there are other factors that ought to be considered for many regions with slip partitioning, such as back arc spreading [*Dewey*, 1980; *Yu et al.*, 1993] and buttressing effects in the forearc [*Beck*, 1991] (deformation ${}_b\vec{V}_c$ and within section c). *Yu et al.* [1993] examined characteristics of slip partitioning along the world's major subduction zones and found that there are linear relationships between earthquake slip vector obliquity (i.e., deflection of earthquake slip vectors from the trench normal) and plate convergence obliquity angles for almost all the subduction zones. They also found that slip partitioning measured by the residual between the earthquake slip vector and plate convergence obliquity is correlated for regions with active back arc spreading and thus inferred that back arc spreading may be an important factor in controlling slip partitioning at subduction zones. However, their model could not give any quantitative analysis, because of the paucity of observational constraints to back arc spreading.

Previous models for slip partitioning have focused on the upper plate deformation and the force balance on the sliver plate. We find that slip partitioning is observed at subduction zones where neither forearc shear faults nor back arc spreading have been found. Because interplate earthquakes occur between the upper and subducting plates, slip partitioning must depend on the tectonic forces on both plates, and the deformation caused by oblique subduction could occur not only in the upper plate, but within the downgoing slab as well. The effects of downgoing slab pull on slip partitioning have been considered only indirectly via slab dip angles in earlier mechanical models [*Beck*, 1991; *McCaffrey*, 1992]. Such effects deserve more exploration. In this study we examine the relationship between slip partitioning, that is, relative motion ${}_d\vec{V}_b$ as in Figure 2, and possible deformation within the downgoing slab caused by forces acting on the slab, particularly the slab pull force in all major subduction zones worldwide for which earthquake data are adequate (Figure 1).

Our model uses two observational parameters: the plate convergence obliquity ϕ, the angle between the directions of plate motion and trench normal, and the earthquake slip vector obliquity ψ, the angle between the directions of earthquake slip vector and trench nor-

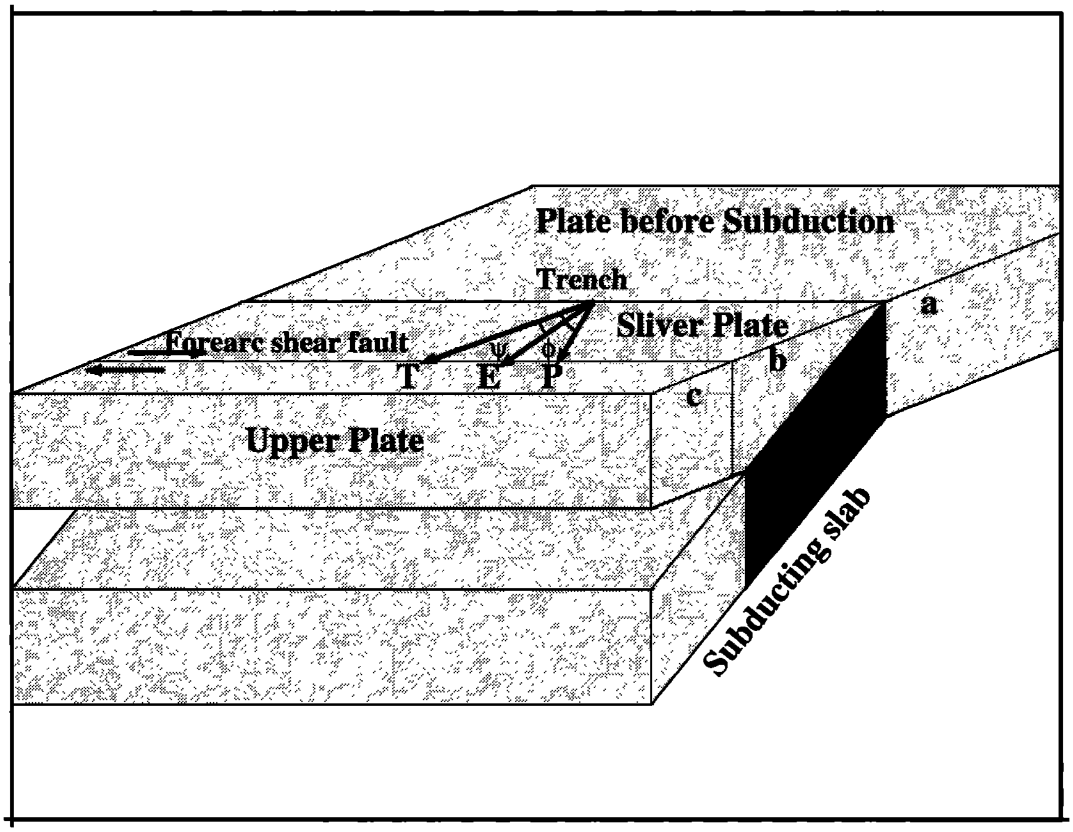

Figure 2. Cartoon showing the (section a) oceanic incoming plate, (section b) sliver plate, forearc shear fault, (section c) upper plate, (section d) subducting slab, and directions of the plate motion $\vec{P}$, trench normal $\vec{T}$, and earthquake slip $\vec{E}$ at a subduction zone (section d). ϕ is the angle between $\vec{P}$ and $\vec{T}$, and ψ the angle between $\vec{E}$ and $\vec{T}$. The shaded region in block (d) is the interplate coupling segment of the slab and may be deformed laterally by oblique subduction.

mal. We propose that for plate convergence obliquity less than the critical value ϕ_{crit} (30° used in this study), earthquake slip vector directions are dependent mainly on slab pull force, which is the major plate driving force at the subduction zones. Slab pull together with the oblique resistance at the interplate surface and the mantle viscous drag at the bottom of the slab causes lateral shear within the slab and the change of the slab trajectory. The value ϕ_{crit} is selected, so that ψ approximately linearly increases with ϕ for $\phi < \phi_{\text{crit}}$ and ψ does not vary rapidly for $\phi > \phi_{\text{crit}}$. As suggested by *McCaffrey* [1992], ϕ_{crit} is considered to be the threshold for the initiation of the arc parallel strike-slip faulting which takes up the plate motion and contributes significantly to rotation of the earthquake slip vectors from the plate motion directions. We establish force balance equation for a segment of the subducting slab at the coupled interface. The dimension of the segment is about the same as the seismogenic zone, thus the forces are the average over the seismogenic zone. We then discuss the roles of those forces to the deformation of the downgoing slab and the consequence to the earthquake slip vector obliquities at subduction zones. Correlation between the earthquake slip partitioning and the calculated slab pull force at various circumstances offers a test of our model.

Data

Selected Interplate Earthquakes

Our data set of interplate earthquake source mechanisms along various subduction zones is assembled from the Harvard Centroid Moment Tensor (CMT) catalog [*Dziewonski et al.*, 1988, and references therein] with following characteristics: (1) seismic moment greater than 1.5×10^{17}N m ($M_w = 5.3$); (2) Harvard CMT depth range within ±50 km of the upper surface of the slab; (3) probable fault plane strike within ±10° of the local trench strike (a larger range of strike direction would include more slip vectors and generally lead to greater scatter, but would not significantly change the average azimuth of the slip vectors [*Liu*, 1993]); (4) probable fault plane dip angle within ±20° of the local slab dip, which is calculated using slab trajectories from *Jarrard* [1986a]. The data selection criteria (3) and (4) are conservative, so that our data set is relatively homogeneous. The final data set includes about 450 interplate earthquakes between January 1977 and

December 1990, with depths up to 80 km, but 20–60 km for most of the events.

We examine the influence of our seismic moment threshold on the selection of interplate earthquakes and find that the azimuthal distribution of the earthquake slip vectors is essentially independent of the earthquake magnitude (see Figure 3a and 3b). We select interplate earthquakes at the subduction zones shown in Figure 1. The subduction zone segmentation used in this study is based on the seismological and tectonic characteristics given by *Jarrard* [1986a]. The code name for each subduction zone segment is listed in Table 1.

The slip vectors for larger earthquakes are usually better constrained than those for smaller earthquakes.

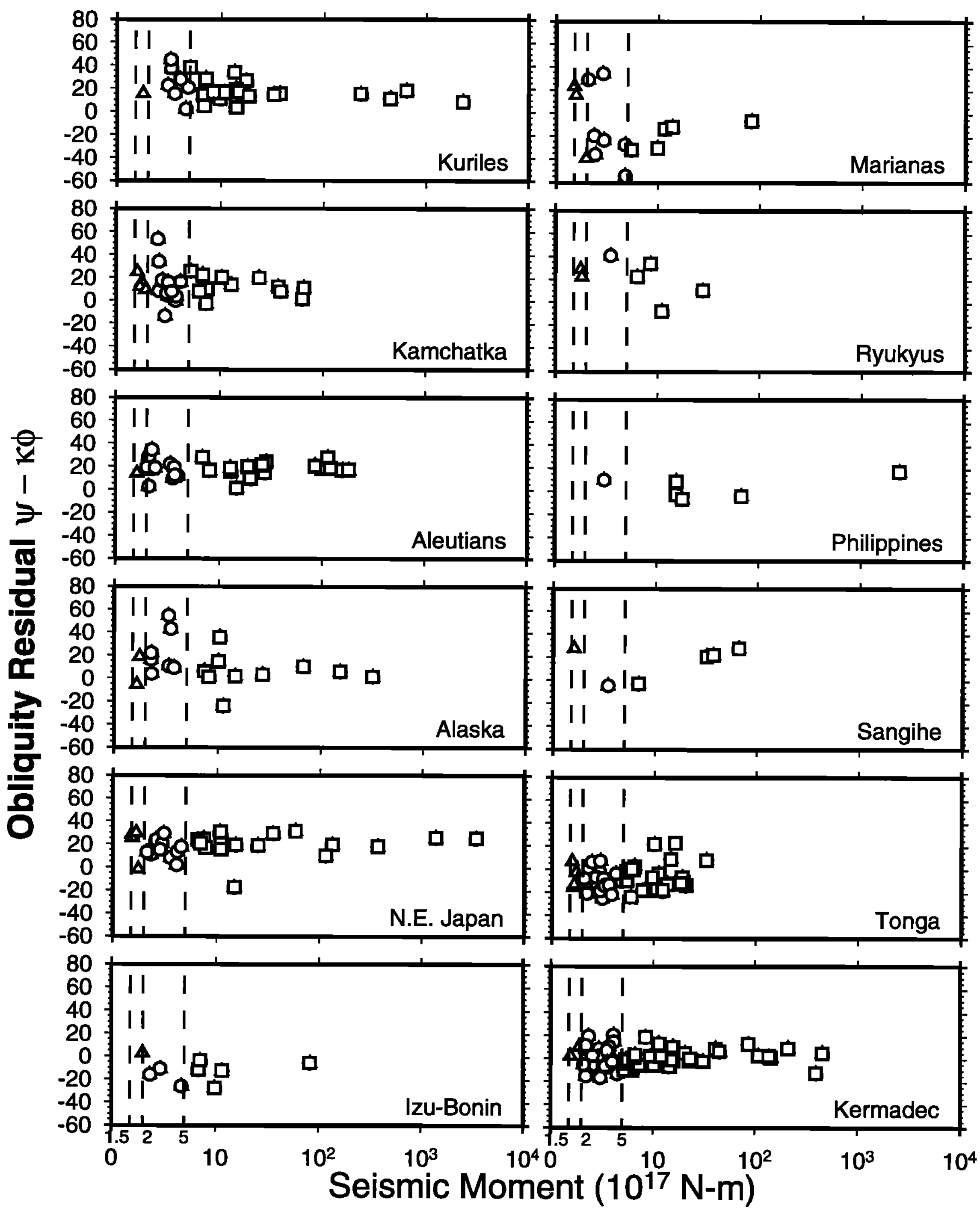

Figure 3. Dependence of obliquity residual $\psi - \kappa\phi$ on seismic moment. Here ϕ is plate convergence obliquity and ψ, earthquake slip vector obliquity. Also, κ is the degree of slip partitioning, defined as $1- < \psi/\phi >$ (see text for detail). Earthquakes of moment between 1.5 and 2.0×10^{17}N m ($5.3 \leq M_w < 5.5$) are marked as triangles, $2.0 - 5.0 \times 10^{17}$N m ($5.5 \leq M_w < 5.8$) as circles, and above 5.0×10^{17}N m ($M_w \geq 5.8$) as squares.

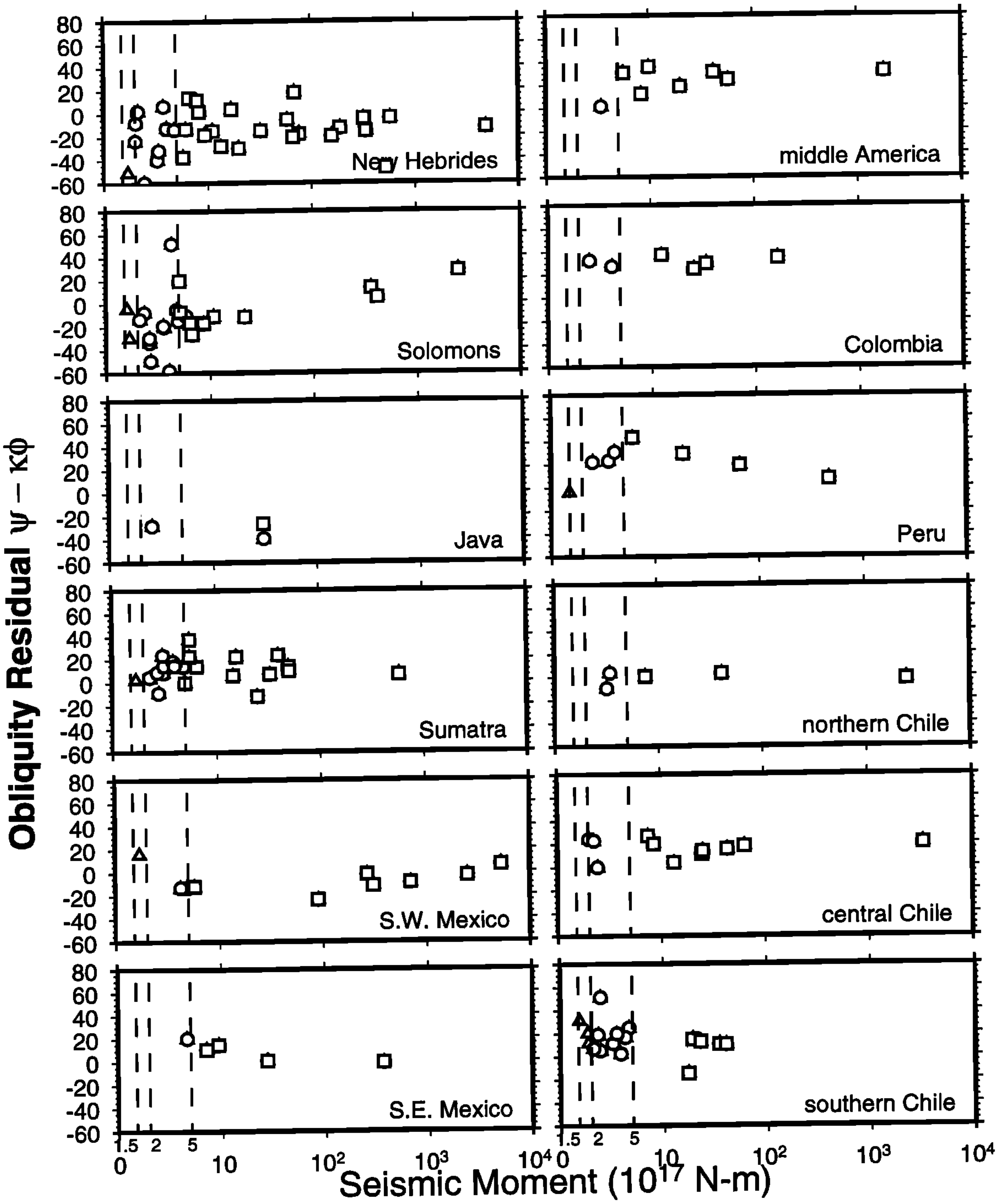

Figure 3. (continued)

A major cause of these uncertainties is the effect of heterogeneities in the upper mantle on the modeling of the body or surface waves for moment tensor inversion [*DeMets*, 1993]. The data we use here are from the Harvard CMT solutions, which are less susceptible to upper mantle heterogeneities. This is because both long period surface and body waves are used simultaneously in the inversions for the earthquake focal mechanisms, and the effects of heterogeneities tend to be reduced [*Ekström and Engdahl*, 1989]. There is no direct estimate for the uncertainty of the earthquake slip vector from the Harvard CMT catalog. However, the uncertainty of moment tensors given there is about 10% in average, which is equivalent to about 5°–10° for the uncertainty of the earthquake slip vector direction.

Relative Plate Motion Directions at Trenches

If a forearc sliver plate is present (Figure 2), the slip vectors of earthquakes indicate the motion of the underthrusting plate with respect to the forearc plate ($_d\vec{V}_b$), not with respect to the major overriding plate. Since

Table 1. Subduction Zone Parameters

Trench Code Name	Trench Full Name	Forearc§ Shear Faults	Upper Plate† Property	Strain† Class	Back Arc‡ Spreading
kerm	Kermadec	No	O	1	—
tong	Tonga	No	O	1	Yes
nheb	New Hebrides	No	O	1	Yes
solo	Solomons	Yes	O	4	—
java	Java	No	C-O	5	No
suma	Sumatra	Yes	C	5	No
sagi	Sangihe	No	O	—	—
phil	Philippines	Yes	C-O	—	Yes
ryuk	Ryukyus	No	C	2	Yes
mari	Marianas	No	O	1	Yes
izub	Izu-Bonin	No	O	2	Yes
nejp	N.E. Japan	Yes	C	6	No
kurl	Kuriles	Yes	C	5	No
kamc	Kamchatka	No	C	5	No
aleu	Aleutians	Yes	O	4	No
alsk	Alaska	No	C	6	No
swmx	S.W. Mexico	No	C	6	No
semx	S.E. Mexico	No	C	6	No
mida	Middle America	No	C	3	Yes
colm	Colombia	Yes	C	6	—
peru	Peru	No	C	6	No
nchl	Northern Chile	No	C	7	No
cchl	Central Chile	No	C	7	No
schl	Southern Chile	Yes	C	5	No

Upper plate property: C, continental; O, oceanic; and C-O, transition between continental and oceanic. Strain class: 1, active back arc spreading; 2, very slow back arc spreading; 3, mildly tensional; 4, neutral or mildly tensional to mildly compressional; 5, mildly compressional; 6, moderately compressional; and 7, very strongly compressional.

† *Jarrard* [1986a].

§ Regional studies referenced by *Jarrard* [1986a] (see text for details).

‡ *Uyeda and Kanamori* [1979].

shear motion rates in forearcs are not well known for most subduction zones, we ignore the effects of ${}_b\vec{V}_c$ in this study. To assess the error caused by the omission, *Jarrard* [1986a] estimated that a strike-slip rate of 10% of the overall plate convergence rate would cause a change of 5.2° in earthquake slip vector direction for plate convergence obliquity of 30°. Strike-slip rates of the forearcs may be less than 10% for most of the subduction zone segments in this study, except for the Aleutians, 25% and Sumatra, 50% [*Jarrard*, 1986a]. The shear motion rate in the forearc can affect slip partitioning in a systematic manner but the result may be minor for most of the subduction zone segments considering that a few degree changes in plate motion direction are comparable to its own uncertainty and to the uncertainty of the slip vector. The above estimate holds if what we know about the strike-slip rates at the subduction zones are true. If not, the forearc shear may not be ignored, and we will have more discussion about this later.

The directions of relative plate motion are calculated for all the selected subduction zones based on Euler vectors given in the NUVEL-1 model [*DeMets et al.*, 1990], except for plate motions between the Philippines and Eurasia plates and the Philippines and Pacific plates. The directions of the plate motion in the Marianas, Izu-Bonin, Ryukyus, Philippines, and Sangihe are calculated based on the Euler vectors given by *Seno et al.* [1987]. *DeMets* [1993] recently tested alternative plate motion models, NUVEL-SZ and NUVEL-G, which are fit to the plate motion data, respectively, excluding subduction zone earthquake slip vectors and excluding both subduction zone and transform fault earthquake slip vectors. He found that NUVEL-SZ and NUVEL-G do not differ significantly from NUVEL-1, except along the boundaries of the Caribbean plate. Thus the NUVEL-1 model is considered sufficiently accurate for our study.

Local Trench Normal Directions

The local trench normal directions are calculated from digitized global tectonic maps of the circum-Pacific Map Project, 1981 (*D. Christensen*, personal communication, 1988). The uncertainty of the trench data is not clearly known, but the trench data we use are quite comparable to the trench locations derived by *Yu et al.* [1993] from the database DBDB5 of 5 min average bathymetry, thus we expect the trench normal directions derived in this study are reasonably reliable. We use the polynomial function of degree N to fit the trench data at each subduction zone. N varies from region to region in order to obtain a locally satisfactory fit. Uncertainty of a few degrees for the trench normal directions is probably a reasonable assessment, based on the misfit of the smoothed trench normal directions and the raw trench data.

Plate Convergence Obliquity and Earthquake Slip Vector Obliquity

Three typical azimuthal distributions of the plate motions, trench normals, and slip vectors of interplate earthquakes are shown in Figure 4 for the Colombia, Tonga, and Marianas subduction zones (other regions are shown in Figure 5a-5d). We see, as a confirmation of the results shown by *Yu et al.* [1993] that earthquake slip vectors tend to follow the directions of plate motion in the Colombia subduction zone which is a strongly coupled region. For Tonga, a moderately coupled subduction zone, earthquake slip vectors are oriented between the directions of plate motion and trench normal. The earthquake slip vectors in the Marianas largely follow the directions of trench normal, a common feature for weakly coupled subduction zones. (The classification of coupling at subduction zones used here is based on the maximum earthquake size criteria of *Kanamori* [1977]).

Given the plate motion vector $\vec{\mathrm{P}}$, trench normal vector $\vec{\mathrm{T}}$, earthquake slip vector $\vec{\mathrm{E}}$ (Figure 2), and the corresponding azimuths, Φ_{P}, Φ_{T}, and Φ_{E}, two basic terms are commonly defined in slip partitioning studies:

$$\phi = |\Phi_{\mathrm{P}} - \Phi_{\mathrm{T}}| \tag{1}$$

and

$$\psi = \begin{cases} \Phi_{\mathrm{E}} - \Phi_{\mathrm{T}}, & \text{if } \Phi_{\mathrm{P}} - \Phi_{\mathrm{T}} \geq 0, \\ -(\Phi_{\mathrm{E}} - \Phi_{\mathrm{T}}), & \text{if } \Phi_{\mathrm{P}} - \Phi_{\mathrm{T}} < 0, \end{cases} \tag{2}$$

where ϕ is the plate convergence obliquity, and ψ is the earthquake slip vector obliquity. $\vec{\mathrm{P}}$ and $\vec{\mathrm{E}}$ usually deviate from $\vec{\mathrm{T}}$ in the same manner, which yields positive sign for ψ. However, we do find a few ψ angles having negative signs. This sign inconsistency indicates that earthquake slip vectors occasionally deviate from the direction normal to the trench in the opposite azimuthal direction from the direction of plate motion. In such cases, ψ does not necessarily reflect the fundamental tectonic significance, but rather may reflect a local stress anomaly or uncertainty of the data. The plots of ψ versus ϕ for all the selected subduction zones are shown as solid and open symbols in Figure 6. Scatter can be seen in almost every subduction zone segment. Solid symbols are earthquakes selected for further analyses by an iterative process which will be elaborated on later in the Results section.

Method

Degree of Slip Partitioning

We define the degree of slip partitioning for a subduction zone as

$$\kappa = 1 - < \frac{\psi}{\phi} >, \tag{3}$$

where $< \psi/\phi >$ is the mean of ψ/ϕ for the subduction zone. Here κ normally ranges between 0 and 1 indicating from zero partitioning to complete partition-

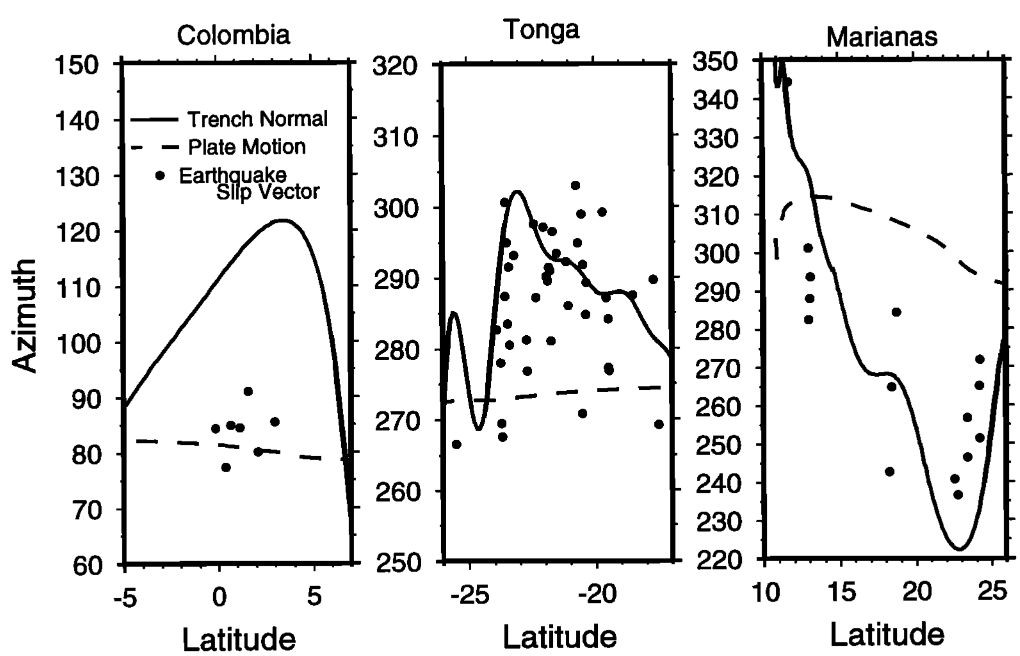

Figure 4. Three typical azimuthal distributions for the plate motion, trench normal, and earthquake slip vectors. Directions of earthquake slip vectors tend to follow the directions of the plate motion at strongly coupled subduction zones (e.g., Colombia); directions of earthquake slip vectors follow the directions of trench normal at weakly coupled subduction zones (e.g., Marianas); directions of the earthquake slip vectors orient between the directions of the plate motion and the trench normal at moderately coupled subduction zones (e.g., Tonga).

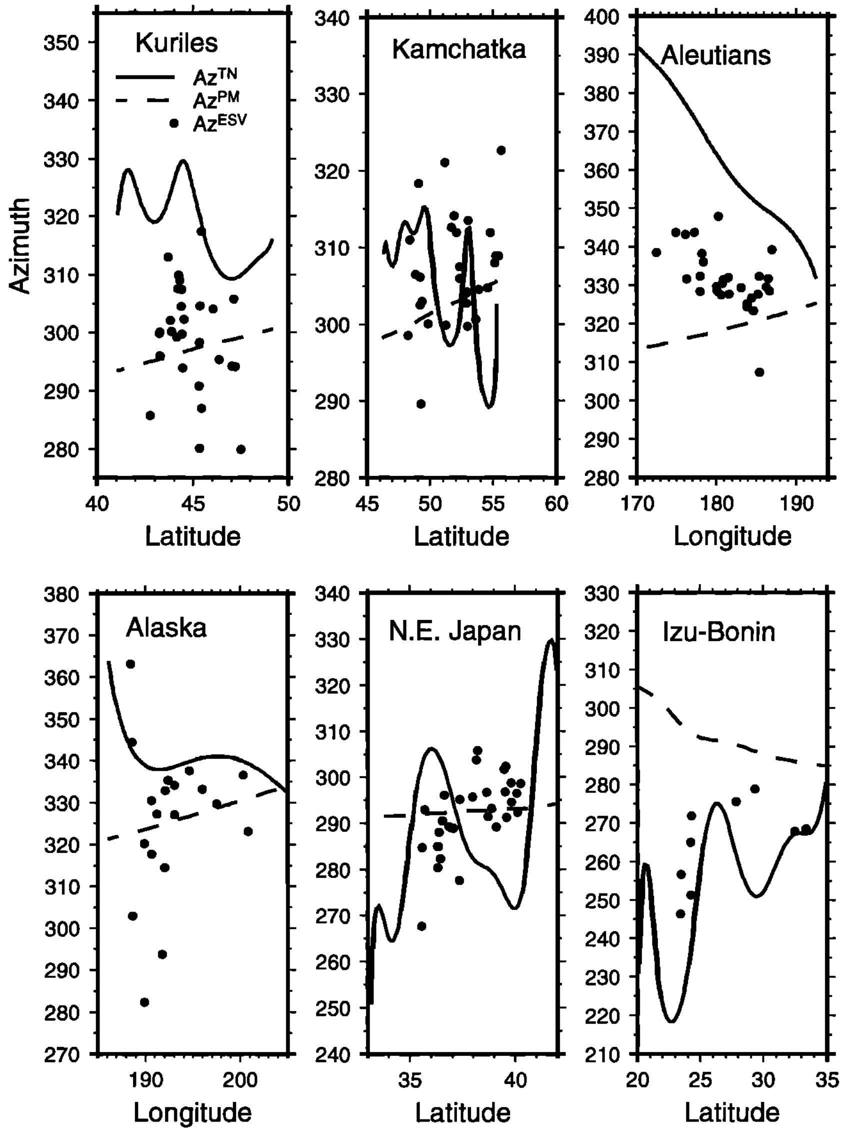

Figure 5. Azimuths of trench normal (Az^{TN}), plate motion (Az^{PM}), and earthquake slip vectors (Az^{ESV}).

ing (Figure 6). This is because slip vectors generally deviate from the plate motion directions towards the trench normal directions [*Fitch*, 1972], corresponding to $\phi > \psi > 0$. For a given ϕ, smaller values of ψ correspond to higher values of κ, that is, greater degree of plate motion partitioning. We examine the correlation between the degree of slip partitioning and slab pull as potential causal factor. This allows us to estimate the degree to which slab pull affects the slip partitioning process.

Calculated Slab Pull Force (F_s)

The slab pull component along the dip direction of the subducting slab can be estimated using the formula

$$F_s = k_1 S^3 {}_aV_c \sin(\delta_I)\left[1 - \exp\left(\frac{k_2}{S^2 {}_aV_c \sin(\delta_I)}\right)\right], \quad (4)$$

where S is the thickness of the lithosphere, ${}_aV_c$ is the plate convergence rate in millimeters per year including back arc spreading, δ_I is the dip angle in the intermediate depth range (i.e., 100–400 km) of the slab, $k_1 = 2.37 \times 10^6$, $k_2 = -1.74 \times 10^5$, and

$$S = \begin{cases} 8.19\sqrt{t}, & \text{for } t \le 70 \text{ Ma}, \\ 91.3 - 74.9\, e^{\left(\frac{-t}{62.8}\right)}, & \text{for } t > 70 \text{ Ma}, \end{cases}$$

where t in Ma is the age of the plate entering the subduction zone. Equation (4) is given by *England and Wortel* [1980] and summarized by *Jarrard* [1986a]. A minor revision is made to replace δ_D (dip angle in the deep depth range) in their formula by δ_I for the sake of self consistency, because δ_I is available for all the selected subduction zones, but δ_D is not.

In (4) the controlling parameters include the convergence rate, slab age, and dip angle. Slab pull can also

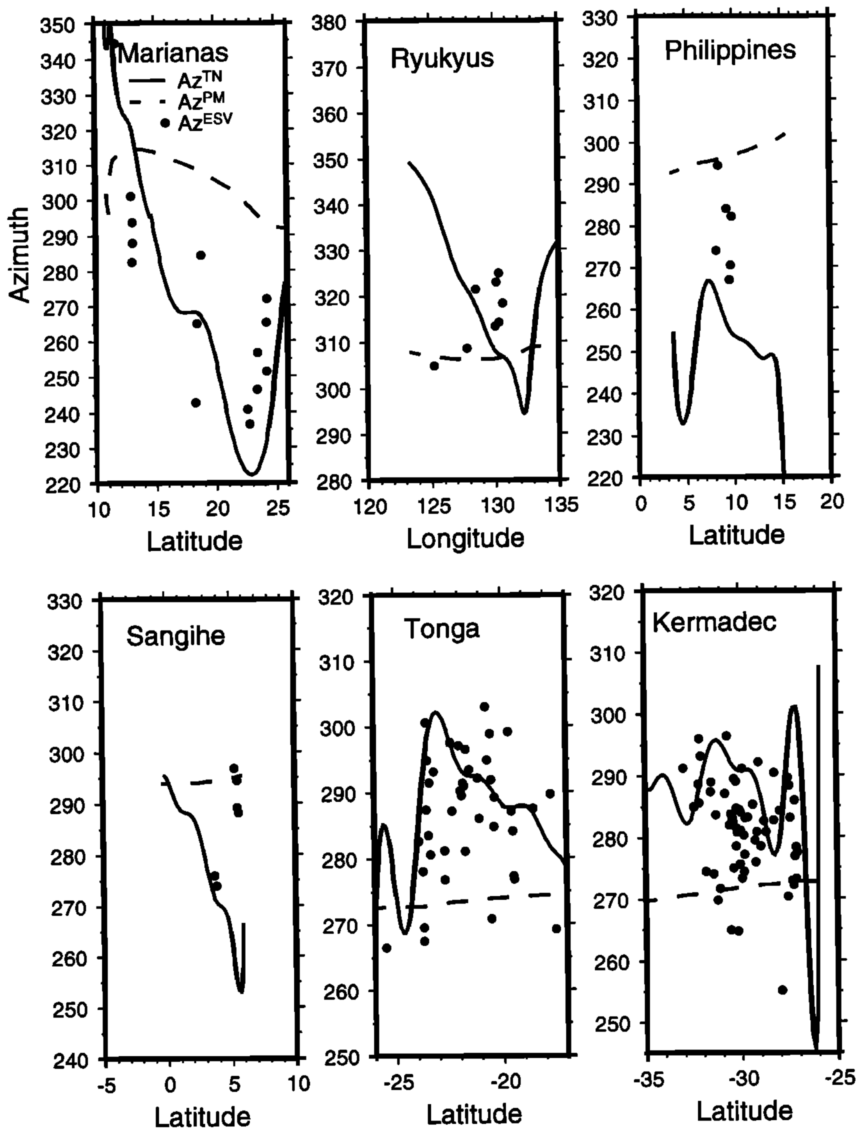

Figure 5. (continued)

be estimated from slab geometry and its density contrast with the surrounding mantle. However, the lack of downdip seismicity at some subduction zones makes the latter estimates less precise. Thus in this study we use *England and Wortel's* formulation (4) to calculate the slab pull. It is not easy to make an accurate estimate of the slab pull force; and there is no exception by using the *England and Wortel's* formulation, since parameters k_1 and k_2 are difficult to estimate precisely. However, their formula can give a better estimate of the relative significance of the slab pull force which is what we would like to use in our later work, because it mainly relies on the relatively better known physical parameters of the slab such as its convergence rate, age, and dip angle. The values of those parameters we use are from *Jarrard*'s study [1986a] which are well compiled. The calculated slab pull for each segment of the subduction zone is listed in Table 2.

Model for Slip Partitioning

Here we propose a model which includes lateral shear of a slab caused by the interplate shear resistance, viscous mantle drag, and slab pull to explain slip partitioning at subduction zones. As the oceanic plate subducts at the trench, the slab is subject to five forces: ridge push, slab pull, frictional resistance (interplate coupling shear) at the upper surface of the slab, viscous resistance at the lower surface of the slab, and lateral compression or extension along trench strike as illustrated in Figure 7. Because the viscous resistance has the same direction as the interplate resistance at the upper surface, practically we can combine them into one in the following discussion for simplicity. In the trench normal direction the plate motion is dependent on the slab pull and the trench normal components of ridge push and frictional resistance. The resultant of those three

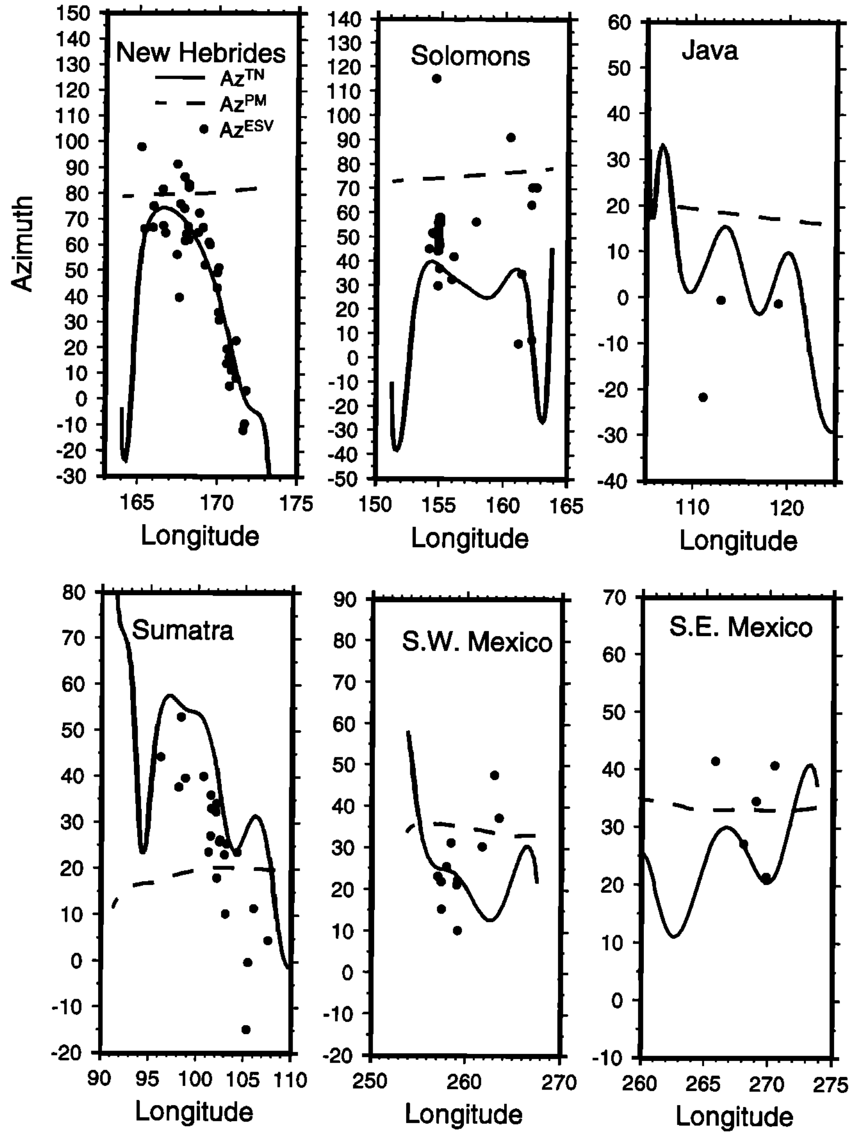

Figure 5. (continued)

forces keeps the slab subducting into the mantle. The trench parallel component of the plate motion is controlled by the along strike gradient of the lateral force and the trench parallel components of the frictional resistance and ridge push. The force balance equations for a segment of the downgoing slab are given as:

$$\begin{cases} F_{cs}\sin\psi' - F_{rp}\sin\phi' = dF_{lg}/dx \\ F_{cs}\cos\psi' - F_{rp}\cos\phi' = F_{sp} \end{cases}, \tag{5}$$

where F_{rp} is the ridge push force, F_{cs} is the interplate resistance, dF_{lg}/dx is the lateral gradient of the along strike force, and F_{sp} is the slab pull force. Here ϕ' and ψ' are the convergence obliquity and earthquake slip vector obliquity projected on the dipping slab surface. For the same oblique angle ϕ', if the slab pull F_{sp} is larger, we know $F_{cs}\cos\psi' - F_{rp}\cos\phi'$ has to be larger. According to *Forsythe and Uyeda* [1975], ridge push F_{rp} is much smaller than F_{sp} and F_{cs} at the trench, therefore $F_{cs}\cos\psi'$ has to be larger, that means a larger F_{cs} and/or smaller ψ'. A larger F_{cs} would impose a greater lateral shear resistance at the slab, making along strike motion more difficult, therefore ψ' smaller. Such frictional resistance is distributed over the whole interplate coupling zone, which makes the plate motion direction gradually turn to the trench normal as the interplate shear continuously applies along with the subduction. A recent study by *Shen* [1995] demonstrated that oblique subduction of a Newtonian fluid slab could show about 30% slip partitioning at 100-km downdip, given reasonable modeling parameters; and the deflection of the obliquity occurs the most in the upper 100-km range.

Figure 8 shows the model predicted slip partitioning effects by *McCaffrey*'s [1992] and by our model. While not including the slab pull in his slip partitioning model, *McCaffrey* [1992] suggested that there is no significant slip partitioning if the plate convergence obliquity ϕ

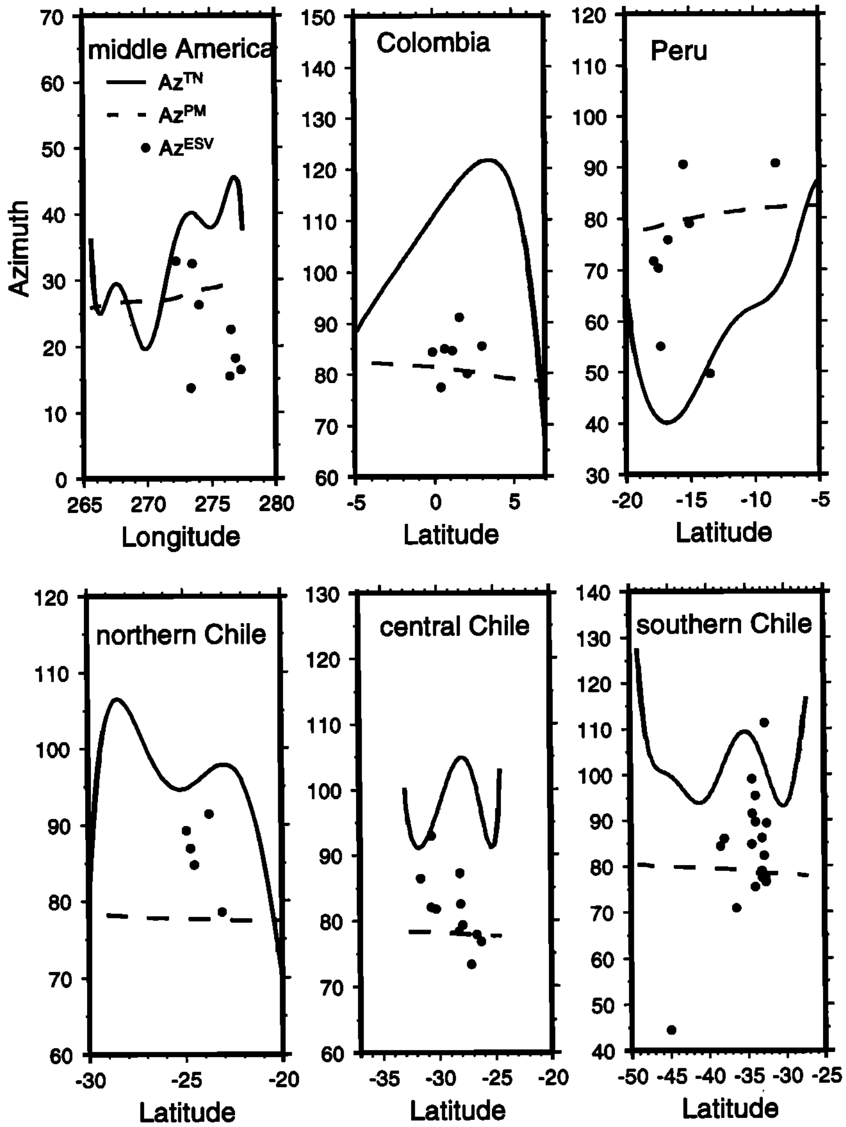

Figure 5. (continued)

is smaller than the critical value ϕ_{crit}. In his model, earthquake slip vector obliquity ψ is approximately the same as the plate convergence obliquity ϕ if $\phi < \phi_{crit}$. When $\phi > \phi_{crit}$, the effect of arc parallel shear force becomes significant, and ψ becomes constant. Our model also predicts a linear relationship between ϕ and ψ, as proposed by *McCaffrey* [1992] and *Yu et al.* [1993], but the coefficient is less than 1.0 due to slab pull effects introduced in our model. Linear coefficients of less than 1.0 can be seen clearly for many subduction zone segments, such as the Kuriles, Aleutians, Alaska, Tonga, Kermadec, New Hebrides, Sumatra, northern Chile, central Chile, and southern Chile (Figure 6). The value b for each subduction zone in Figure 6 is the least squares slope of the fit (dashed lines) to the data (solid symbols only) for $\phi \leq 30°$. The average value of the slope in Figure 6 is about 0.5±0.2. For some subduction zone segments, such as Kamchatka, northeastern Japan, the Ryukyus, and middle America subduction zones the slopes of ψ versus ϕ are greater than 1.0. This phenomenon will be discussed in the Discussion section.

We examine the average change of the plate motion direction over the extent of the seismogenic zone (50–200 km) along slab dip by evaluating the mean of $\phi - \psi$ at each subduction zone segment. For all subduction zone segments where the average slip vector rotates from the plate motion direction toward the trench normal direction, we find that the rotation angle is 3°–14° (with an average of 8°).

If the lateral shear exists in the slab, it may be reflected in the focal mechanisms of intraplate earthquakes. We examine this phenomena in the Tonga subduction zone (Figure 9). All the selected intraplate earthquakes ($M_w \geq 6.0$ and 60–190 km from the trench) demonstrate strike slip faulting mechanisms (Harvard CMT solutions); and one of the nodal planes for each selected intraplate earthquake indicates the lat-

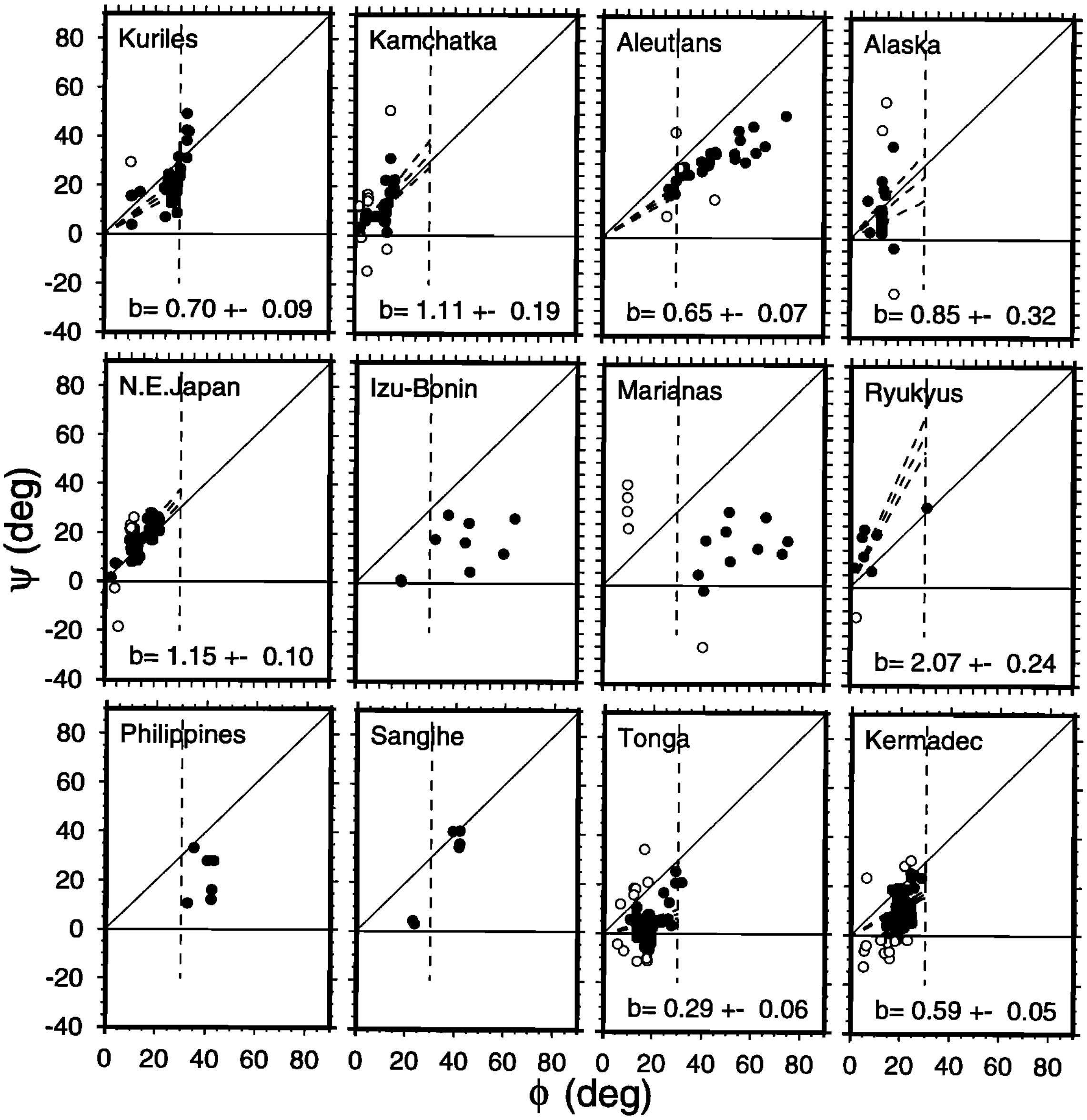

Figure 6a. Distributions of the plate convergence obliquity ϕ and the earthquake slip vector obliquity ψ at the Kuriles, Kamchatka, Aleutians, Alaska, northeasten Japan, Izu-Bonin Marianas, Ryukyus, Philippines, Sangihe, Tonga, and Kermadec subduction zone segments. Solid symbols are selected events for further analysis through a filtering process of two standard deviation of the mean ψ/ϕ (see the text). Open symbols are those falling out of the two standard deviation range. Three dashed lines are the least squares fits, with the slope b and its uncertainty to the data of $\phi \leq 30°$ (solid symbols). The vertical dashed line indicates $\phi = 30°$.

eral shear direction consistent with the shear direction (i.e., the lower part of the slab shears against the upper part) supposedly induced by slab pull. This suggests that lateral shear associated with slab pull effect is possible in the slab.

The average rate of slab motion will be more or less constant during subduction over a time period much longer than the underthrust earthquake cycle. Change of the plate subduction direction introduces along trench lateral shear in the slab, caused by the trench parallel component of the slab resistance applied on the entire interplate coupling surface. The shear strain (we adopt engineer shear strain here) associated with the range of slip vector rotation is between 5–25%, with the average of 15%. Harvard CMT focal mechanisms show that in many cases the lateral (trench parallel) strain is observable, though the downdip stress generally dominates the lithospheric faulting process [*Burbach and Frohlich*, 1986]. The subducting slab is generally under nonzero lateral strain if it is to maintain a constant dip angle in the mantle. *Press* [1968] showed that the lateral strain in the slab can be zero only if the slab dip angle is half of the radius of the trench arc. *Burbach and Frohlich* [1986] estimated one-dimensional strain in the slab along the 10-Ma isochrone between adjacent points that were originally at the trench at the same time. The plate convergence vector and slab dip angle revealed by subduction zone seismicity were used to obtain the 10-Ma isochrone. From their estimates, the slab can be deformed laterally by amount

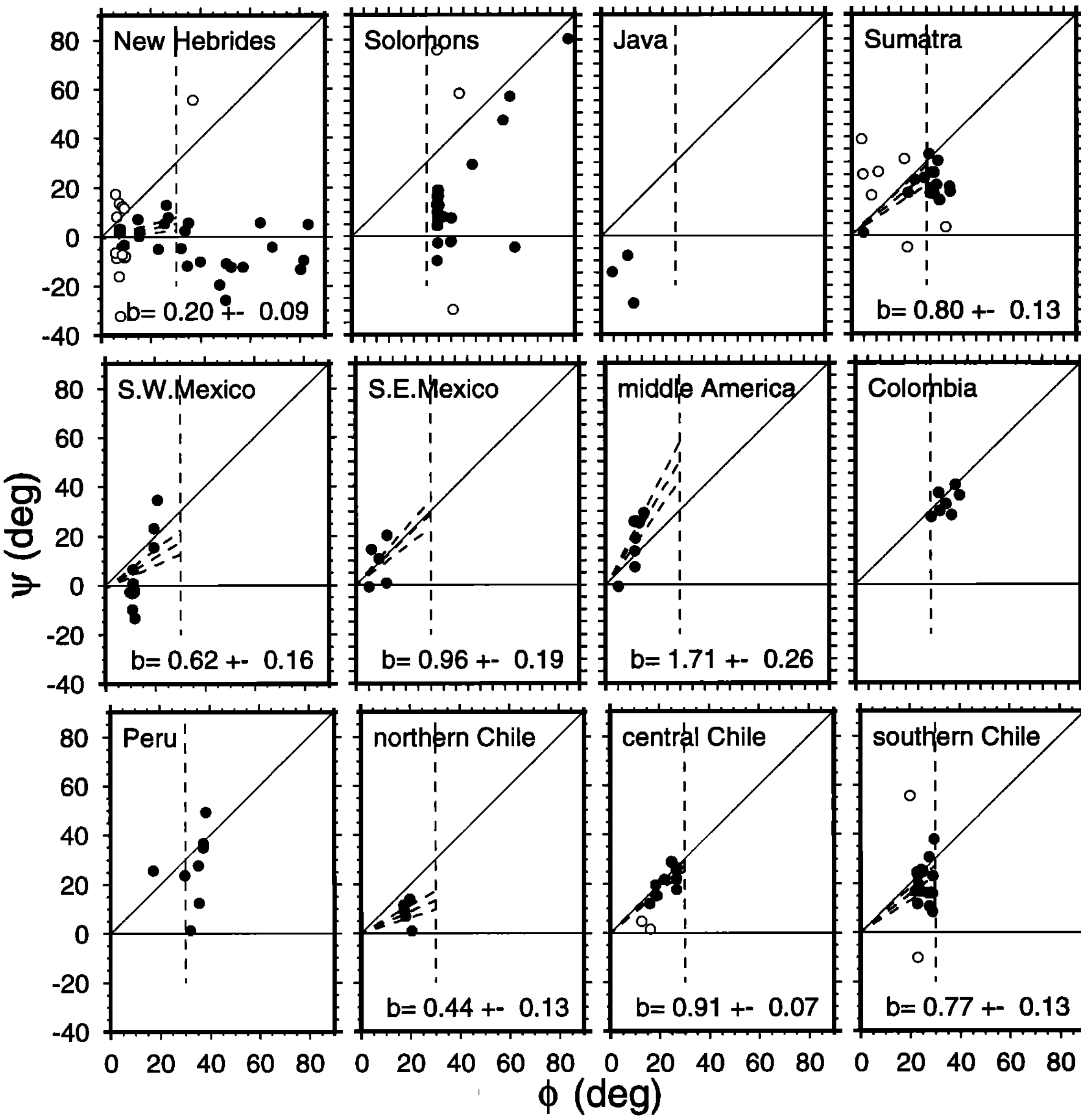

Figure 6b. Distributions of the plate convergence obliquity ϕ and the earthquake slip vector obliquity ψ at the New Hebrides, Solomons, Java, Sumatra, southwestern Mexico, southeastern Mexico, middle America, Colombia, Peru, northern Chile, central Chile, and southern Chile subduction zone segments. Other details as in Figure 6a.

of 10–15%. Therefore the slab is not absolutely rigid and perhaps 10–15% shear strain in the slab is possible, if the appropriate forces are applied, as suggested by the modeling work of *Shen* [1995]. The amount of shear strain predicted by the earthquake slip vector rotation is based on the earthquakes occurring within 50 to 200–km distance along the slab dip direction. The distance range over which slip vectors change directions can be larger, but it is expected that the significant change of slip vector directions occurs within the first 100–300 km along slab dip direction. In Tonga subduction zone, the deep slab material moves relatively to the south by about 500 km, indicating systematic shear deformation in the slab. This has been interpreted by the driving of the horizontal shear flow in the mantle [*Giardini and Woodhouse*, 1986]. *Fischer and Jordan* [1991] estimated the seismic strain rate orientation tensors and inferred that the deep slab in Tonga is experiencing 50% thickening due to arc parallel deformation. Our suggested mechanism of simple shear in the slab requires the shear strain which is quite comparable to that predicted by the slab geometry [*Burbach*

Table 2. Calculated Slab Pulls and Their Dependent Subduction Zone Variables

Trench Code Name	Plate Age† A_s, Ma	Convergence Rate‡ $_aV_c$, cm/yr	Intermediate Dip†* δ_I, deg	Calculated F_s, 10^{12} N/m
kerm	113	10.5	30	25.23
tong	120	12.5	28	26.51
nheb	52	9.0	44	16.78
solo	50	12.0	42	17.59
java	138	8.2	21	—
suma	55	6.2	19	9.68
sagi	—	—	—	—
phil	—	4.6	41	—
ryuk	49	3.0	23	5.18
mari	155	10.3	24	26.64
izub	146	7.6	28	25.00
nejp	130	9.9	19	23.17
kurl	119	8.7	28	24.11
kamc	90	8.8	25	20.24
aleu	54	6.0	31	12.59
alsk	46	6.3	13	5.65
swmx	15	5.9	25	1.88
semx	14	7.2	18	1.52
mida	23	6.5	38	5.40
colm	15	6.8	26	2.25
peru	45	8.2	13	6.93
nchl	82	10.0	21	18.80
cchl	48	9.8	14	9.21
schl	26	9.7	16	4.50

† *Jarrard* [1986a].
‡ *Chase* [1978].
* Intermediate dip angle determined by the average dip of the slab above 100 km depth.

and Frohlich, 1986] and deep slab shear deformation [*Giardini and Woodhouse*, 1986; *Fischer and Jordan*, 1991].

The relative plate motion at the trench may be accommodated by the trench parallel shear in the slab, as well as the shear in the forearc plate. Those two mechanisms of slip partitioning may be the end-members of such a process. Actual slip partitioning may be a combination of both mechanisms. However, to start with a simple model, we consider only the slab pull influence which causes trench parallel shear in the slab and thus deviates the earthquake slip vector direction away from the plate motion direction. For plate convergence obliquity less than 30°, using only slab shear mechanism may not be a bad approximation, since the forearc shear faults are not likely to be well developed, and the slab shear may be the dominant mechanism for slip partitioning.

Results

Degree of Slip Partitioning (κ) on Slab Pull and Existence of Forearc Shear Faults

We examine the degree of slip partitioning, $\kappa = 1 - \langle \psi/\phi \rangle$, for all the trenches and its dependency on the

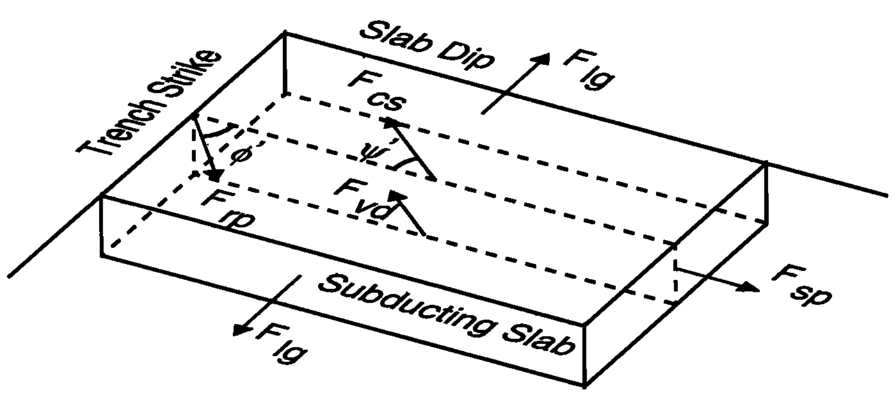

Figure 7. Force balance for a segment of a subducting slab. Slab pull F_{sp}, ridge push F_{rp}, interplate coupling shear F_{cs}, viscous mantle drag F_{vd}, and lateral stress gradient dF_{lg}/dx are the major forces applied on the segment of a subducting slab (slant view). The scale of the segment covers the seismogenic zone. Here ϕ' and ψ' are the obliquities measured on the slant view.

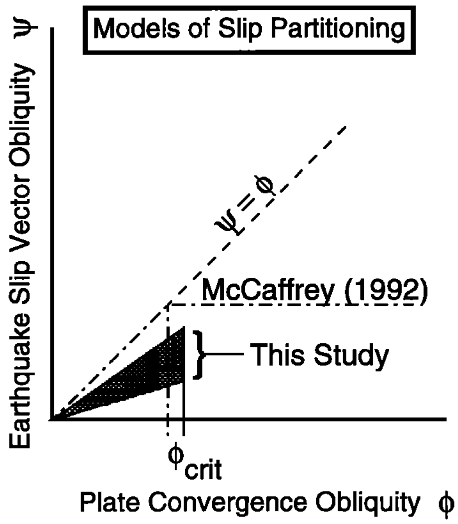

Figure 8. Model predicted slip partitioning by *McCaffrey* [1992] and this study. *McCaffrey* suggested $\psi = \phi$ for convergence obliquity less than a critical value; and $\psi =$ constant when plate convergence exceeds that critical value. We propose $\psi = a\phi$ for convergence obliquity less than the critical value. Here a is less than 1.0, which is associated with the slab pull effect on the earthquake slip vector obliquity. Data in Figure 6 suggests $a = 0.5 \pm 0.2$.

degree of slab pull and the existence of forearc shear faults. To ensure that the calculated value κ is stable and representative for the data, we filter out the data points with ψ/ϕ deviations from the mean $< \psi/\phi >$ being larger than two standard deviations. Through several iterations, all remaining data points are within two standard deviations from $< \psi/\phi >$. The ψ/ϕ data for each subduction zone segment are shown in Figure 10. The earthquakes which are selected through filtering are shown as solid symbols in Figure 6 for each subduction zone segment. Open symbols in Figure 6 are those eliminated by filtering. The Ryukyus and Java are excluded in the analysis because standard deviations of ψ/ϕ for those segments are very large. The Philippines and Sangihe segments are also excluded because no reliable plate age, convergence rate, or plate dip angle are available for estimating the slab pull forces in these two regions.

The existence or absence of forearc shear fault in each region is listed in Table 1. Most references are from *Jarrard* [1986a] and are reviewed briefly below. The classification for the existence of forearc shear faults is mainly based on studies of Pleistocene strike-slip faults, and occasionally on earthquake focal mechanisms. There is no reported geological and seismological evidence suggesting forearc shear faults in the Tonga, Kermadec, Sangihe, Ryukyus, Marianas, Kamchatka, southwestern Mexico, southeastern Mexico, and middle America subduction zones. There is no evidence of forearc shear faults inland of selected segments of the New Hebrides [*Dubois et al.*, 1978], Java [*Katili*, 1970], Izu-Bonin [*Kaizuka*, 1975; *Karig and Moore*, 1975; *Ichikawa*, 1980], Alaska [*Lathram et al.*, 1974], Peru [*Stauder*, 1975; *Philip and Megard*, 1977], north and central Chile [*Brown et al.*, 1993; *Scheuber et al.*, 1990]. Forearc shear faults are observed inland of several segments, such as the Kuriles [*Kaizuka*, 1975; *Ichikawa*, 1980], Aleutians [*Comier*, 1975; *Geist et al.*, 1988], northeastern Japan [*Ichikawa*, 1980], Philippines [*Fitch*, 1972], Solomons [*Coleman and Hackman*, 1974], Sumatra [*Fitch*, 1972; *Katili*, 1970], Colombia [*Campbell*, 1974], and southern Chile [*Cembrano et al.*, 1992]. We admit that our classification of the regions with and without forearc shear faults may not be reliable for every region. However, we just use the best knowledge as we can, and our final results are based on the statistics of all the regions, not on the reliability of classification for one particular region.

The existence of active back arc spreading for the subduction zone segments are summarized by *Uyeda and Kanamori* [1979] and listed in Table 1. The type of structures (continental or oceanic) for the upper plate for each segment is also listed in Table 1.

We analyze the relationship between the degree of slip partitioning and the slab pull and/or forearc shear faults for the full range of plate convergence obliquities. We also examine these relationships for values of ϕ_{crit} other than 30° to address the influence of forearc shear faults and slab pull on the degree of slip partitioning. For each range of ϕ we determine the correlation coefficient R and obtain the slope b. The larger values of R usually coincide with the higher values of the best fit slope b and higher T value (defined as b/σ) (Table 3).

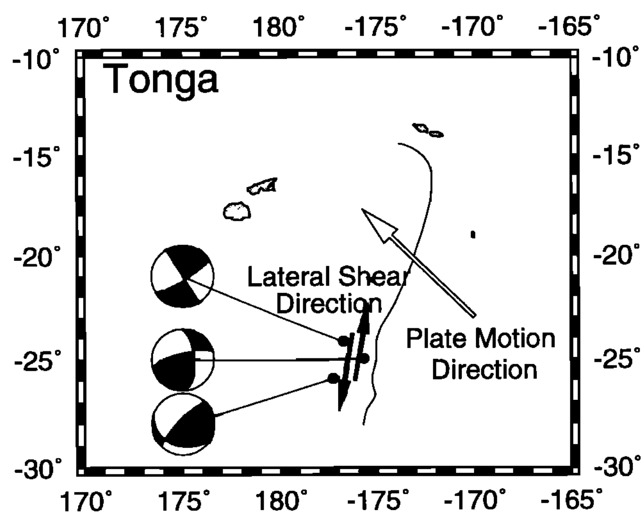

Figure 9. Map view of the selected $M_w \geq 6.0$ intraplate earthquakes (solid symbols) and their focal mechanisms at the Tonga subduction zone. The open arrow indicates the relative plate convergence direction, which is oblique to the trench normal. Solid arrows indicate the direction of lateral shear in the slab induced by the slab pull effect on the oblique convergence. One of the nodal planes for each earthquake demonstrates the trench parallel component of strain consistent with the lateral shear direction supposedly induced by slab pull.

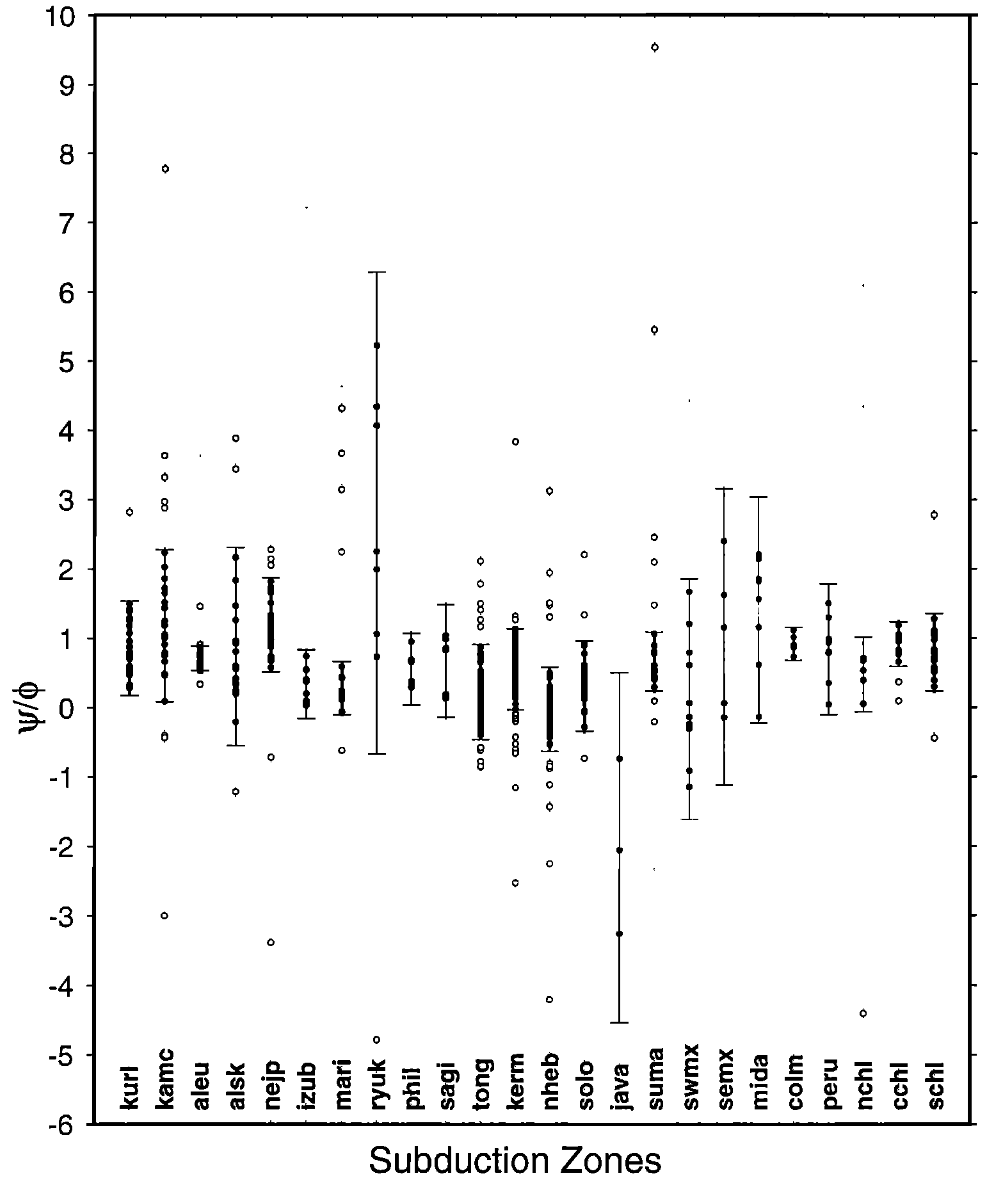

Figure 10. Values of ψ/ϕ at each major segment of the subduction zone. The bar shown in each segment is the two standard deviation of the mean of ψ/ϕ. Most subduction zone segments have reasonably small ranges of the two standard deviations, and 90% of the ψ/ϕ (solid symbols) fall into such ranges. Data in solid symbols will be used in further analyses. Open symbols are those whose values of ψ/ϕ fall out of the range of the two standard deviation in each subduction zone.

In general, we find that regions without forearc shear faults show larger b value and more significant correlation than the regions with forearc shear faults do (Figure 11a-11c). A further examination reveals that most significant b value (0.024 ± 0.014) comes from the regions without forearc shear faults and with $\phi < 30°$ (Figure 11b). This suggests that at those regions, slab pull is likely an important factor controlling the degree of slip partitioning. Forearc shear faults may play an important role in controlling the degree of slip partitioning for $\phi > 30°$ in addition to slab pull; but for $\phi \leq 30°$, the general relationship between slab pull and the degree of slip partitioning is less affected. For the regions with forearc shear faults, we do not have many data points and they are scattered, thus the estimation of the b value suffers from large uncertainty. However, for

Table 3. Fitting Slope b of κ (Degree of Slip Partitioning) versus Calculated Slab Pull F_s

	0-90° $b\pm\sigma$*		0-30° $b\pm\sigma$		30-90° $b\pm\sigma$	
	R†	T‡	R	T	R	T
Regions with shear faults	-0.004±0.014		-0.004±0.017		-0.005±0.023	
	-0.13	-0.28	-0.14	-0.24	-0.13	-0.22
Regions without shear faults	0.020±0.012		0.024±0.014		0.015±0.027	
	0.44	1.67	0.47	1.71	0.36	0.56
Total of all regions	0.014±0.009		0.017±0.012		0.013±0.017	
	0.32	1.56	0.35	1.42	0.28	0.76

* Fitting slope b and its uncertainty σ.
† Correlation coefficient R.
‡ $T = b/\sigma$.

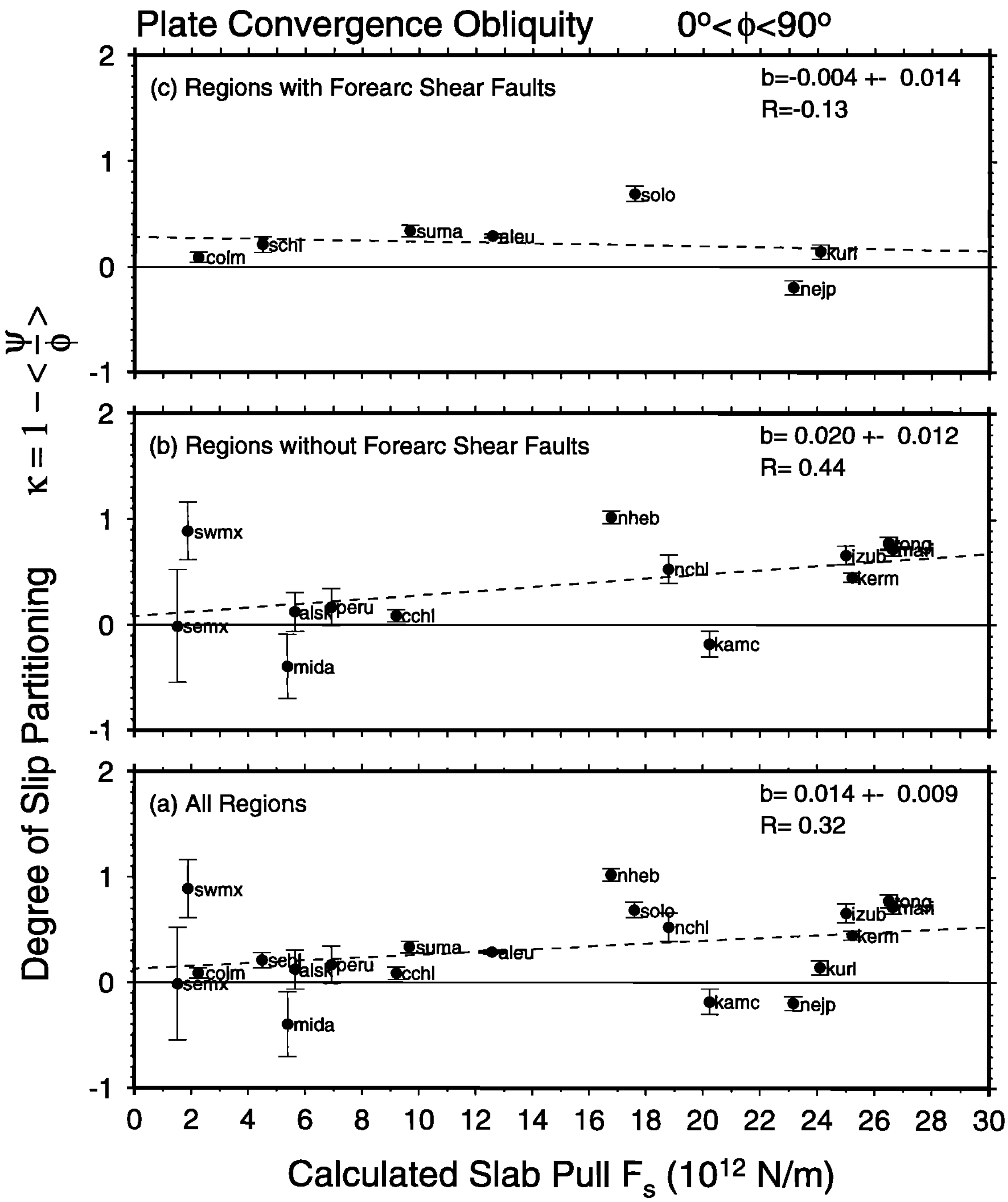

Figure 11a. Fit of the degree of slip partitioning κ calculated for $0 < \phi < 90°$ versus the calculated slab pull F_s for (*a*) all regions, (*b*) regions without forearc shear faults, and (*c*) regions with forearc shear faults. Here b is the slope of the fit. R is the correlation coefficient for the given data set.

the regions with forearc shear faults, possible influence of slab pull forces on slip partitioning still cannot be ruled out.

Discussion

Regions of ψ Versus ϕ Slope Greater Than 1.0

Net mantle downdip resistance might be indicated by the slope of ψ versus ϕ greater than 1.0 in Figure 6 for the Kamchatka, northeastern Japan, Ryukyus, and middle America subduction zones. In general, net mantle downdip resistance is not impossible for (seismically) strongly coupled subduction zones, because slab pulls for those regions are thought to be less important than those at moderately or weakly coupled subduction zones. However, it is not clear how large the net mantle downdip resistance should be.

Relationship of Slip Partitioning With Dip Angle

Previous models attribute slip partitioning to the role of forearc plate deformation. A typical relationship de-

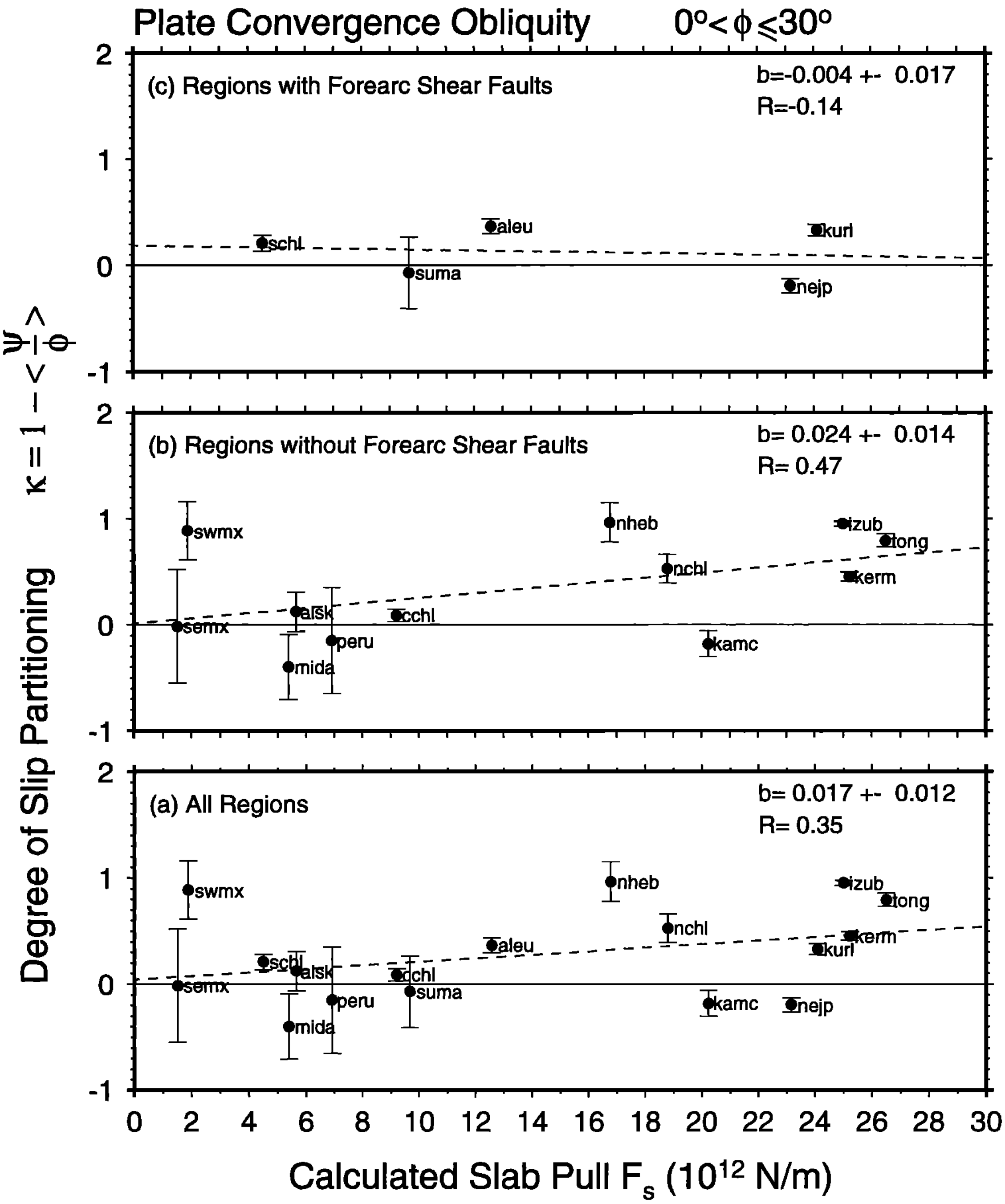

Figure 11b. Fit of the degree of slip partitioning κ calculated for $0 < \phi \leq 30°$ versus the calculated slab pull F_s. Other details as in Figure 11a.

rived based on such a model was given by *McCaffrey* [1992] as

$$\sin\psi_{max} = Z_s\tau_s'\sin\delta / Z_t\tau_t', \tag{6}$$

where $\psi_{\max}$ is the maximum slip obliquity angle, δ is the slab dip angle, Z_s and Z_t are the vertical depths of the interplate coupling and the forearc shear fault, and τ_s' and τ_t' are the maximum shear stresses on the coupling surface and on the forearc shear fault. This relationship suggests that if factor $Z_s\tau_s'/Z_t\tau_t'$ does not vary much from region to region, $\psi_{\max}$ is approximately linear to dip angle δ. Because $\psi_{\max}$ is a measure of the slip partitioning, that is, higher $\psi_{\max}$ means less slip partitioning, this relationship implies that slip partitioning would be less as dip angle gets larger. However, as we find in Table 4 and Figure 12, κ correlates most strongly with the dip angle δ, especially for $\phi \leq 30°$; which suggests higher slip partitioning when dip angle is getting larger, just the opposite as what Equation (6) implies. One might argue that the parameters Z_s, τ_s', Z_t, and τ_t' may vary region by region, thus a simple linear assumption between $\phi_{\max}$ and δ may not be valid. However, an opposite correlation, as what the data suggest, would require factor $Z_s\tau_s'/Z_t\tau_t'$ proportional to $1/\sin^2\delta$. This proportionality is hard to explain without introducing other partitioning mechanism(s).

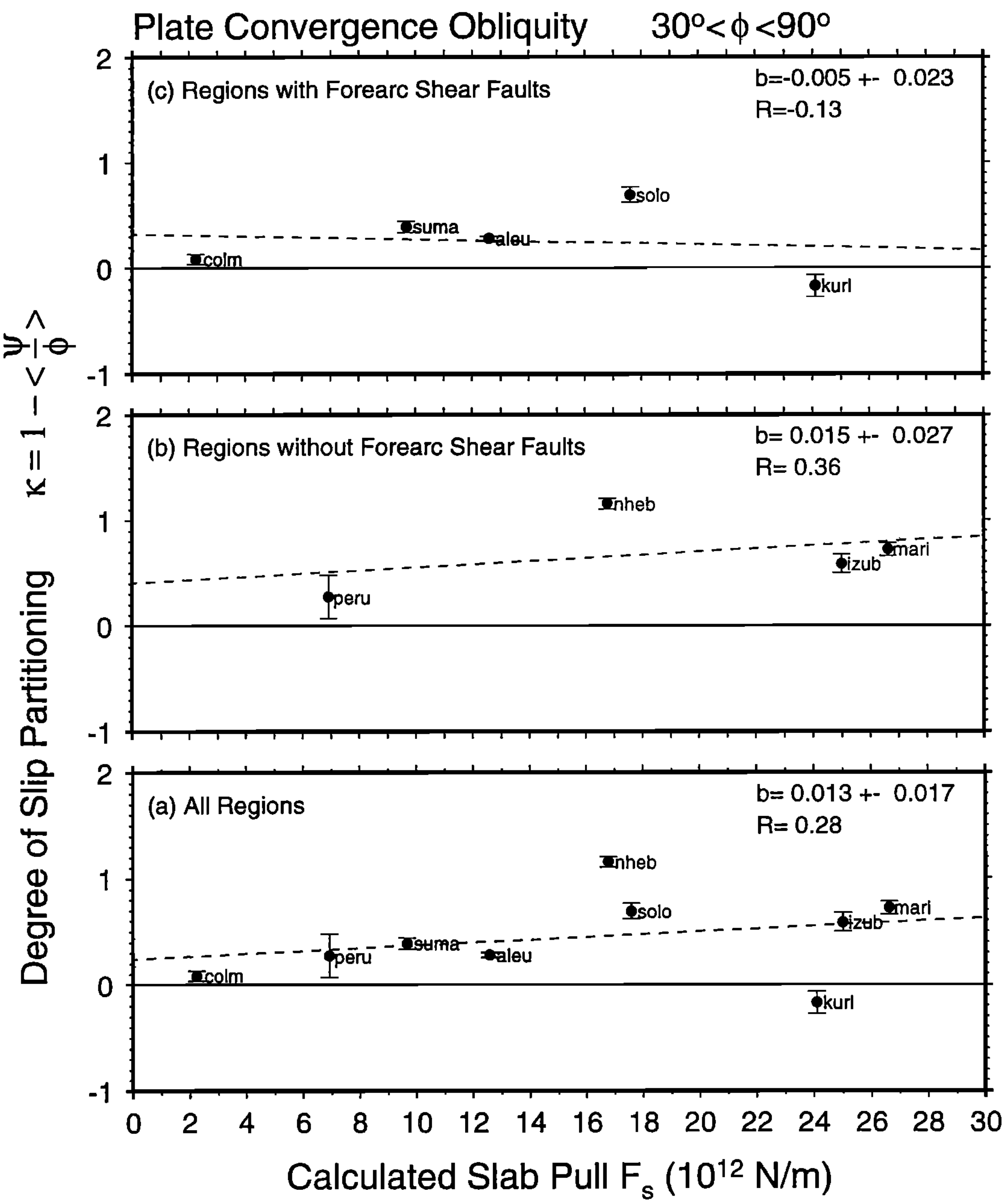

Figure 11c. Fit of the degree of slip partitioning κ calculated for $30° < \phi < 90°$ versus the calculated slab pull F_s. Other details as in Figure 11a.

Table 4. Fitting Slope b of κ (Degree of Slip Partitioning) versus Plate Convergence Rate, Age, and Dip Angle

	0-90° $b \pm \sigma$*		0-30° $b \pm \sigma$		30-90° $b \pm \sigma$	
	R†	T‡	R	T	R	T
κ vs. rate	0.058±0.044		0.045±0.058		0.086±0.068	
	0.30	1.32	0.20	0.78	0.43	1.26
κ vs. age	0.002±0.002		0.003±0.003		0.001±0.003	
	0.22	1.00	0.27	1.00	0.08	0.33
κ vs. dip	0.015±0.009		0.020±0.012		0.018±0.011	
	0.37	1.67	0.41	1.67	0.50	1.64

* Fitting slope b and its uncertainty σ.
† Correlation coefficient R.
‡ $T = b/\sigma$.

Correlation of Slip Partitioning With Plate Convergence Rate

A recent analysis of slip partitioning by *McCaffrey* [1993] suggested that great subduction zone earthquakes ($M_w \geq 8.0$) are highly correlated with small slip vector residual ($\phi - \psi$) in the locality of the great earthquakes and high rates of plate convergence. We examine the correlation of slip partitioning κ in our study with plate convergence rates and we do not find such a strong correlation (Table 4 and Figure 12). The correlation between the degree of slip partitioning and the age of the plate is not large either. In all the obliquity ranges, slip partitioning κ is more strongly correlated

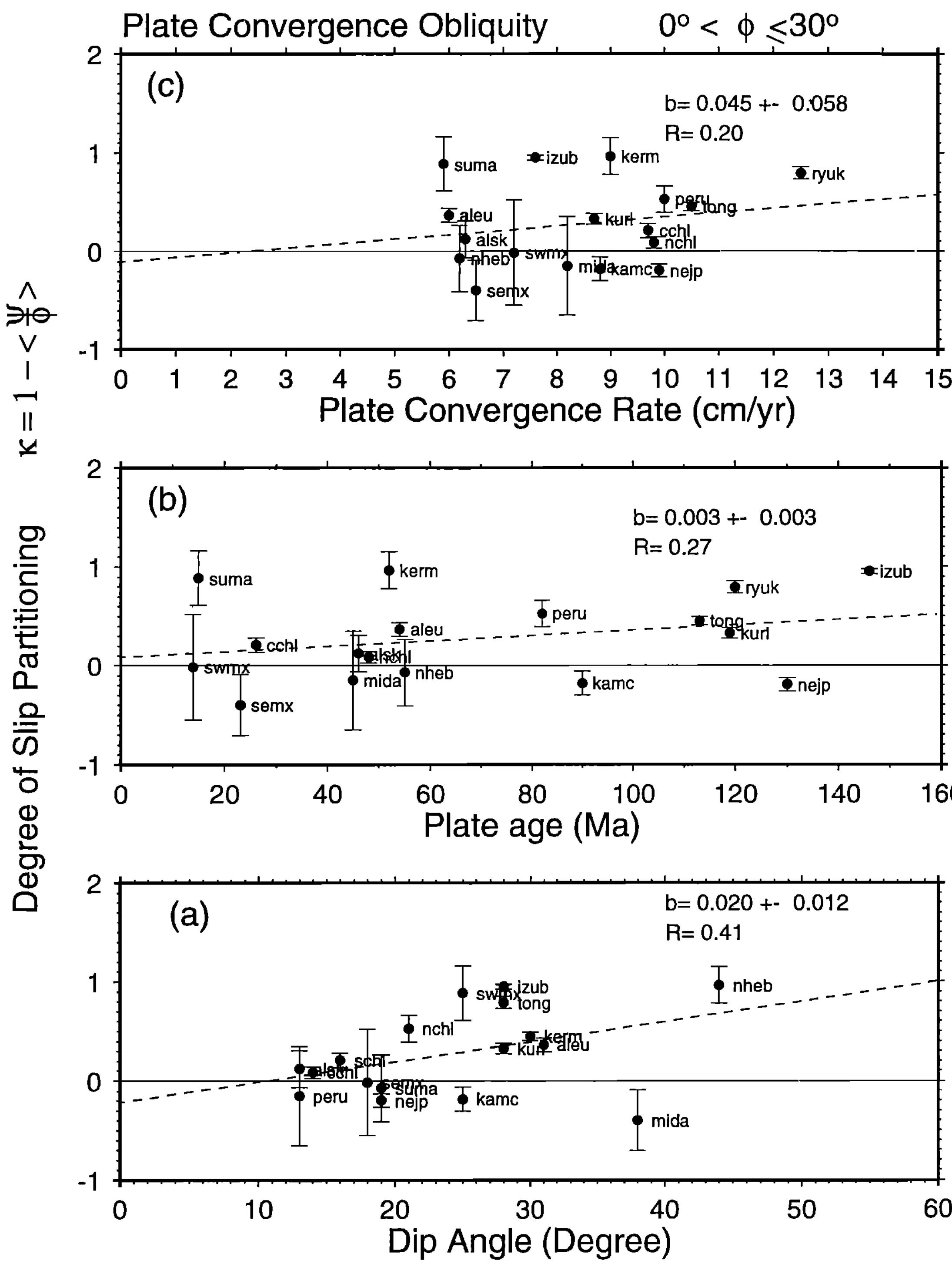

Figure 12. Fit of the degree of slip partitioning κ calculated for $0 < \phi \leq 30°$ versus (*a*) dip angle, (*b*) age of the plate, and (*c*) plate convergence rate. Here b is the slope of the fit. R is the correlation coefficient for the given data set. The correlation coefficient is the largest for dip angle among the three cases.

with the dip angle than with the convergence rate and with age of the plate (Table 4 and Figure 12). This is not too surprising, because dip angle is more correlated with the slab pull force than other parameters are.

Dependency of Slip Partitioning on Back Arc Spreading

Some previous studies [*Dewey*, 1980; *Jarrard*, 1986b; and *Yu et al.*, 1993] suggested that back arc spreading may play important role in slip partitioning. This mechanism, however, is difficult to explain the general pattern of slip partitioning, which shows linear increase along with the subduction obliquity. Moreover, the rate and direction of back arc spreading is difficult to measure, and such data usually suffer from large uncertainty. Recent development in application of the Global Positioning System (GPS) provides opportunities to acquire accurate measurements of back arc spreading at subduction zones. There has been few regions with good back arc spreading measurements because GPS technique requires years of observation. The GPS study in Tonga [*Bevis*, 1993], the only geodetic measurement we know, resulted 22±2 cm/yr for the relative convergence rate between the oceanic plate and the forearc plate and 16±2 cm/yr for back arc spreading rate. The angle between the two vectors is about $15°-16°$ (*M. Bevis*, personal communication, 1993). Using these measurements, the direction of relative motion between the oceanic plate and the forearc plate is deflected by about 33° from the plate motion direction between the oceanic plate and the major upper plate (equivalent to NUVEL-1) toward trench normal. If such correction is made for Tonga, we find that the predicted plate convergence obliquity is deflected counter clockwise from the trench normal rather than clockwise as the slip vector obliquities are for most earthquakes. This is very difficult to explain, therefore so far we do not perform any correction of back arc spreading effect in this study.

Conclusions

We propose a new model for slip partitioning at subduction zones, that includes slab pull as an additional parameter to explain slip partitioning. In this model the slab is pulled down by gravitational pull normal to the trench strike. The along strike component of the oblique subduction is gradually dissipated by the interplate coupling resistance and the mantle shear as the slab subducts, causing a lateral shear in the slab which makes the slab motion rotate toward the trench normal. Interplate earthquake slip directions ψ at 24 subduction zones are studied against the relative plate convergence directions ϕ. A good correlation is found for 20 subduction zone segments, between the mean degree of slip partitioning $\kappa = 1 - <\psi/\phi>$ and the slab pull F_s calculated from the formula of *England and Wortel* [1980], for the overall range of plate convergence obliquity. For $\phi \leq 30°$, the slope of the best fit line for the degree of slip partitioning κ versus the calculated slab pull F_s is the maximum among all the ranges of ϕ for the regions without forearc shear faults, and is different significantly from zero. This suggests that slab pull plays an important role in controlling earthquake slip partitioning, especially for the regions where no arc parallel shear faults are developed and $\phi \leq 30°$.

Acknowledgments. We are grateful to Heidi Houston, for introducing the topic of slip partitioning, for providing the dataset of global subduction zone earthquakes, and for helpful discussions; to Thorne Lay, Jiajun Zhang, Ru-Shan Wu, Rob Coe, and Susan Schwartz, for critical review of the text, comments, and suggestions. We also thank the Associate Editor of JGR Solid Earth and two reviewers, Myrl E. Beck, Jr., and Robert McCaffrey, for their helpful comments and suggestions. This research was partially supported with facilities from the W. M. Keck Foundation. Contribution 230, W.M. Keck Seismological Laboratory, Institute of Tectonics, University of California, Santa Cruz.

References

Beck, M.E.,Jr., On the mechanism of tectonic transport in zones of oblique subduction, *Tectonophysics, 93*, 1-11, 1983.

Beck, M.E.,Jr., Model for late Mesozoic-early Tertiary tectonics of coastal California and western Mexico and speculations on the origin of the San Andreas fault, *Tectonics, 5*, 49-64, 1986.

Beck, M.E.,Jr., Coastwise transport reconsidered: Lateral displacements in oblique subduction zones, and tectonic consequences, *Phys. Earth Planet. Inter., 68*, 1-8, 1991.

Bevis, M., Geodetic observations of convergence and backarc spreading in the S.W. Pacific (abstract), *Eos Trans. AGU, 74(43), Fall Meet. Suppl.*, 60, 1993.

Brown M., F. Diáz, and J. Grocott, Displacement history of the Atacama fault system 25°00'S-27°00'S, Northern Chile, *Geol. Soc. Am. Bull., 105*, 1165-1174, 1993.

Burbach, G.V., and C. Frohlich, Intermediate and deep seismicity and lateral structure of subducted lithosphere in the Circum-Pacific region, *Rev. Geophys., 24*, 833-874, 1986.

Campbell, C.J., Colombian Andes, in *Mesozoic-Cenozoic Orogenic Belts*, edited by A.M. Spencer, pp.705-724, Scottish Academic, Edinburgh, Scotland, 1974.

Cembrano, J., M.E. Beck, R.F. Burmester, C. Rojas, A. Garcia, and F. Herve, Paleomagnetism of lower cretaceous rocks from east of the Liquine-Ofqui fault zone, southern Chile - Evidence of small in-situ clockwise rotations, *Earth Planet. Sci. Lett., 113*, 539-551, 1992.

Coleman, P.J., and B.D. Hackman, Solomon Islands, in *Mesozoic-Cenozoic Orogenic Belts*, edited by A. M. Spencer, pp.453-461, Scottish Academic, Edinburgh, Scotland, 1974.

Comier, V.F., Composite focal mechanism solution of the Near Islands (Aleutian Islands) earthquakes of February 2, 1975 (abstract), *Eos Trans. AGU, 56*, 393, 1975.

DeMets, C., R.G. Gordon, D.F. Argus, and S. Stein, Current plate motions, *Geophys. J. Int., 101*, 425-478, 1990.

DeMets, C., Earthquake slip vectors and estimates of present-day plate motions, *J. Geophys. Res., 98*, 6703-6714, 1993.

Dewey, J.F., Episodicity, sequence and style at convergent plate boundaries, the continental crust and its mineral deposits, *Geol. Assoc. Can. Spec. Pap., 20*, 553-573, 1980.

Dubois, J., F. Dugas, A. Lapouille, and R. Louat, The troughes at the rear of the New Hebrides inland arc: Possible mechanisms of formation, *Can. J. Earth Sci., 15*, 351-360, 1978.

Dziewonski, A.M., G. Ekström, J.E. Franzen, and J.H. Woodhouse, Global seismicity of 1981: Centroid-moment tensor solutions for 542 earthquakes, *Phys. Earth Planet. Inter., 50*, 155-182, 1988.

Ekström, G., and E.R. Engdahl, Earthquake source parameters and stress distribution in the Adak Island region of the central Aleutian Islands, Alaska, *J. Geophys. Res., 94*, 15,499-15,519, 1989.

England, P., and R. Wortel, Some consequences of the subduction of young slabs, *Earth Planet. Sci. Lett., 47*, 403-415, 1980.

Fischer, K.M., and T.H. Jordan, Seismic strain rate and deep slab deformation in Tonga, *J. Geophys. Res., 96*, 14,429-14,444, 1991.

Fitch, T.J., Plate convergence, transcurrent faults, and internal deformation adjacent to southeast Asia and the western Pacific, *J. Geophys. Res., 77*, 4432-4460, 1972.

Forsyth, D., and S. Uyeda, On the relative importance of the driving forces, *Geophys. J. R. Astron. Soc. 43*, 163-200, 1975.

Geist, E.L., J.R. Childs, and D.W. Scholl, The origin of summit basins of the Aleutian Ridge: Implications for block rotation of an arc massif, *Tectonics, 7*, 327-341, 1988.

Giardini, D., and J.H. Woodhouse, Horizontal shear flow in the mantle beneath the Tonga arc, *Nature, 319*, 551-555, 1986.

Ichikawa, M., Some problems in the focal mechanism in and near Japan, *Geophys. Mag., 39*, 1-22, 1980.

Jarrard, R.D., Relations among subduction parameters, *Rev. Geophys., 24*, 217-284, 1986a.

Jarrard, R.D., Terrane motion by strike-slip faulting of forearc slivers, *Geology, 14*, 780-783, 1986b.

Jones, C.H., and S.G. Wesnousky, Variations in strength and slip rate along the San Andreas fault system, *Science, 256*, 83-86, 1992.

Kaizuka, S., A tectonic model for the morphology of arc-trench systems, especially for the echelon ridge and mid-arc faults, *Jpn. J. Geol. Geogr., 45*, 9-28, 1975.

Kanamori, H., Seismic and aseismic slip along subduction zones and their tectonic implications, in *Island Arcs Deep Sea Trenches and Back-Arc Basins, Maurice Ewing Series, Vol. 1*, edited by M. Talwani and W.C. Pittman, pp.163-174, AGU, Washington D. C., 1977.

Karig, D.E., and G.F. Moore, Tectonic complexities in the Bonin Arc system, *Tectonophysics, 27*, 97-118, 1975.

Katili, J.A., Large transcurrent faults in Southeast Asia with special reference to Indonesia, *Geol. Rundsch., 59*, 581-600, 1970.

Lathram, E.H., et al., Alaska, in *Mesozoic-Cenozoic Orogenic Belts*, edited by A.M. Spencer, pp.563-589, Scottish Academic, Edinburgh, Scotland, 1974.

Liu, X., Studies of shallow inter- and intraplate earthquakes and mechanical models of subduction zone dynamics, *Ph.D dissertation, Univ. of Calif., Santa Cruz*, 1993.

McCaffrey, R., Oblique plate convergence, slip vectors, and forearc deformation (abstract), *Eos Trans. AGU, 71*, 1590, 1990.

McCaffrey, R., Slip vectors and stretching of the Sumatran forearc, *Geology, 19*, 881-884, 1991.

McCaffrey, R., Oblique plate convergence, slip vectors, and forearc deformation, *J. Geophys. Res., 97*, 8905-8915, 1992.

McCaffrey, R., On the role of the upper plate in great subduction zone earthquakes, *J. Geophys. Res., 98, 11,953-11,966*, 1993.

Michael, A.J., Energy constraints on kinematic models of oblique faulting: Loma Prieta versus Parkfield-Coalinga, *Geophys. Res. Lett., 17*, 1453-1456, 1990.

Philip, H., and F. Megard, Structural analysis of the superficial deformation of the 1969 Pariahuanca earthquakes (central Peru), *Tectonophysics, 38*, 259-278, 1977.

Press, F.C., Curvature of island arcs, *Nature, 220*, 363-363, 1968.

Scheuber, E., and P. Andriessen, The kinematic and geodynamic significance of the Atacama fault zone, Northern Chile, *J. Struct. Geol., 12*, 243-257, 1990.

Seno, T., T. Moriyama, S. Stein, D.F. Woods, C. DeMets, D.F. Argus, and R.G. Gordon, Determination of the Philippine Sea plate motion (abstract), *Eos Trans. AGU, 68*, 1474, 1987.

Shen, Z.-K., Oblique subduction of a Newtonian fluid slab, in press, *Pure Appl. Geophys.*, 1995.

Stauder, W., Subduction of the Nazca plate under Peru as evidenced by focal mechanisms and by seismicity, *J. Geophys. Res., 80*, 1053-1064, 1975.

Uyeda, S., and H. Kanamori, Back-arc opening and the mode of subduction, *J. Geophys. Res., 84*, 1049-1061, 1979.

Walcott, R.I., Geodetic strains and large earthquakes in the axial tectonic belt of North Island, New Zealand, *J. Geophys. Res., 83*, 4419-4429, 1978.

Yu, G., S.G. Wesnousky, and G. Ekström, Slip partitioning along major convergent plate boundaries, *Pure Appl. Geophys.*, 140, 183-210, 1993.

X. Liu, Institute of Geophysics and Planetary Physics, University of California, Los Angeles, CA 90095-1567. (e-mail: xliu@igpp.ucla.edu)

K. C. McNally, Institute of Tectonics, University of California, Santa Cruz, CA 95064. (e-mail: redmiata@rupture.ucsc.edu)

Z.-K. Shen, Dept. of Earth and Space Sciences, University of California, Los Angeles, CA 90095-1567. (e-mail: zshen@hercules.ess.ucla.edu)

(Received November 17, 1994; revised November 17, 1994; accepted March 13, 1995.)